# THERMODYNAMICS OF 1:2 SODIUM BORATE MINERALS

By

LAURA SUZANNE RUHL

A THESIS PRESENTED TO THE GRADUATE SCHOOL
OF THE UNIVERSITY OF FLORIDA IN PARTIAL FULFILLMENT
OF THE REQUIREMENTS FOR THE DEGREE OF
MASTER OF SCIENCE

UNIVERSITY OF FLORIDA

2008

To my family, who have kept my inquisitive spirit and thirst for knowledge alive, always encouraging me, and giving me strength.

ACKNOWLEDGMENTS

First and foremost, I thank the chair of my committee, Phil Neuhoff, for all of his time and all of the knowledge he has bestowed upon me throughout my time as his student. I would also like to thank my committee members, Ellen Martin and Guerry McClellan, for their time and support in my academic endeavors. I thank Jie Wang and Gökce Atalan for their help in the lab, for many scientific discussions and support. I also thank Derrick Newkirk for his unending encouragement and support. Major thanks go to my parents and siblings for always being there to help in any endeavor and their never-ending support and love. Lastly, I appreciate all of the never-ending encouragement from my friends and family. The National Science Foundation funded this project.

TABLE OF CONTENTS

LIST OF TABLES

LIST OF FIGURES

Abstract of Thesis Presented to the Graduate School
of the University of Florida in Partial Fulfillment of the
Requirements for the Degree of Master of Science

THERMODYNAMICS OF 1:2 SODIUM BORATE MINERALS

By

Laura Suzanne Ruhl

December 2008

Chair: Phil Neuhoff
Major: Geology

The stability of borate minerals is an important consideration for assessing biogeochemical processes in primordial and extant Earth-surface environments, in addition to many industrial applications. Borate minerals are found in a variety of environments from playas to evaporite deposits and serve as the most important industrial source of boron used in glass production, fire retardation, and cleaning purposes. Despite the geological and industrial importance of borate minerals, their phase stability and formation remains poorly constrained. In the present study, the thermodynamic properties of borax [$Na_2B_4O_5(OH)_4 \bullet 8H_2O$], tincalconite [$Na_2B_4O_5(OH)_4 \bullet 2.667H_2O$], kernite [$Na_2B_4O_6(OH)_2 \cdot 3H_2O$], and the reactions between them were assessed by thermogravimetric analysis (TGA), differential scanning calorimetry (DSC), hydrofluoric (HF) acid solution calorimetry, X-ray powder diffraction (XRPD), and equilibrium observations. Observations of equilibrium between borax and tincalconite were conducted as a function of temperature and relative humidity (RH) using saturated salt solutions. Mass changes in TGA and isotherm measurements confirm the stoichiometry of tincalconite to be $Na_2B_4O_5(OH)_4 \bullet 2.667H_2O$. The minimum relative humidity of borax equilibrium is 64.92% at 298.15, 74.68% at 313.15K, and 89.19% at 328.15K. The maximum relative humidity in equilibrium with tincalconite increases from 52.89% at 298.15K to 71.00% at 313.15K to 80.7%

at 328.15K to 79.85% at 338.15K. At 338.15K and 95% humidity the sodium borate deliquesced. The increase in the equilibrium constant for the dehydration reaction from borax to tincalconite is consistent with an enthalpy of dehydration (to water vapor) at 323.15K of -55.3 +/- 2.0 kJ/mol of $H_2O$. This is also consistent with the enthalpy of dehydration determined by HF solution calorimetry of -54.33 +/- 0.24 kJ/mol of $H_2O$ and by DSC of -55.6kJ +/- 1.1 kJ/mol of $H_2O$. The enthalpy of dehydration from borax to kernite and tincalconite to kernite determined by HF calorimetry was -56.8 kJ/mol and -1.96 kJ/mol respectively. These results, along with heat capacities for borax, tincalconite, and kernite determined by DSC and molar volumes determined by XRPD, were used to assess the thermodynamic properties of borax dehydration as a function of temperature and pressure. The resulting phase diagram is consistent with geologic observations of Na-borate stability, indicating that in the $Na_2B_4O_7 \bullet H_2O$ system borax is the primary precipitate and stable at earth's surface conditions. Tincalconite is metastable under most of these conditions and kernite is the result of secondary mineralization. Tincalconite holds a small stability field at 298.15K, therefore making it stable at surface conditions.

# CHAPTER 1
# INTRODUCTION

Although boron is relatively scarce in the Earth's crust (twenty-seventh in abundance with an average content of 15 ppm; Anovitz and Grew, 1996), its aqueous and solid phase speciation play a critical role in biogeochemical processes. Seawater is enriched in boron relative to the crust, and acid-base equilibria involving boric acid are an important secondary influence on seawater pH (Dickson, 1990; Krauskopf and Bird, 1995). Despite its relatively low abundance, boron is an important accessory constituent of many rocks formed through hydrothermal, diagenetic, and metamorphic processes (Leeman and Sission, 1996) occurring dominantly as borosilicate minerals such as tourmaline (Anovitz and Grew, 1996). At Earth's surface, boron occurs most often in borate anion-based salts formed during evaporation and subsequent diagenesis of playa evaporite deposits (Anovitz and Grew, 1996). Surficial borate deposits serve as the most important industrial source of boron used in glass production, fire retardation, and cleaning purposes. They have also been observed to stabilize ribose, possibly playing a role in the beginning of life on Earth (Ricardo et al., 2004).

Despite their wide geologic and industrial importance, the stability of borate minerals remains poorly constrained. The present study addresses this issue through an integrated thermodynamic study of the stability of the Na-borate minerals, borax, tincalconite, and kernite that employs a combination of equilibrium, thermal analysis, and calorimetric methods. The following sections of this chapter explore previous observations of the geologic occurrence and stability of these minerals. This discussion raises several critical questions that form the basis of the research described in later chapters.

## Mineralogy and Crystal Chemistry of Na-Borates

Boron can form three- or four-coordinated borate groups, denoted as $B\Phi_3$ and $B\Phi_4$, respectively ($\Phi$: $O^{2-}$ or $OH^-$) (Kemp, 1956). It is the most electronegative element in its group, resembling a non-metal, like carbon, rather than the Group III metals (Kemp, 1956). Kemp (1956) also reports that crystalline borates structurally resemble the silicates, therefore just as the SiO4 tetrahedra can link together in complex silicates, so can the BO3 triangles.

Borax, tincalconite, and kernite all consist of a borate-anion based formula with 1:2 Na:B ratios, but differ in their degree of hydration (Table 1-1). Borax [$Na_2B_4O_5(OH)_4 \cdot 8H_2O$] is a primary evaporite phase that often is pseudomorphed by the isostructural but less hydrous phase tincalconite $Na_6[B_4O_5(OH)_4]_3 \cdot 8H_2O$ (Pabst and Sawyer, 1948;Christ and Garrels, 1959) when exposed to a dry atmosphere. Borate structures contains corner-sharing $B\Phi_3$ and $B\Phi_4$ polyhedra that polymerize to from sheets, chains, or frameworks (Burns et al., 1995). Table 1-1 lists the number of triangularly coordinated ($B\Phi_3$) or tetrahedrally coordinated ($B\Phi_4$) borate ions in each of the minerals in this investigation (Burns et al., 1995). Borax and tincalconite each contain a polyanion with two borate triads and two borate tetrahedrons polymerized to form the structures shown in Figures 1-1 and 1-2, respectively (Burns et al., 1995; Levy and Lisensky, 1978; and Luck and Wang, 2002). Their identical polyanion structures allow for easy transition from one to the other with relatively low activation energy (Christ and Garrels, 1959). Kernite [$Na_2B_4O_6(OH)_2 \cdot 3H_2O$] is structurally distinct due to its intricate chain of borate polyanions. Formation of kernite from either tincalconite or borax requires higher activation energy, and is therefore considerably slower and is not readily reversible (Christ and Garrels, 1959). Figure 1-3 reveals the complexity of the kernite structure compared to borax and tincalconite (Grice et al., 1999).

Compositional relations similar to those exhibited by the 1:2 Na- borates are exhibited by both Ca- and NaCa-borates. The calcium borates follow a sequence very similar to the sodium

borates with myerhofferite [$Ca_2B_6O_6(OH)_{10}•2H_2O$], inyoite [$Ca_2B_6O_6(OH)_{10}•6H_2O$], and colemanite [$Ca_2B_6O_{11}•5H_2O$] differing only in their respective degrees of hydration. NaCa borates also mimic the Na borates, although with only two hydration states. Ulexite [$NaCaB_5O_6(OH)_6•5H_2O$] and probertite [$NaCaB_5O_7(OH)_4•3H_2O$] are the NaCa high hydrates equivalent to borax and kernite, respectively.

## Geological Occurrence of Na-borate Minerals

Most of the borate deposits mined today are from fossil deposits formed thousands to millions of years ago. Searles Lake and Clear Lake (in California) are two borate deposits that are currently forming (Bowser, 1965). Searles Lake is currently undergoing mining in which the salt brine is pumped out from beneath a salt crust on the lake and left to evaporite, leaving behind the valued minerals (Bixler and Sawyer, 1957). Many deposits have a variety of other minerals accompanying the Na-borates (Bowser, 1965). Some of the common minerals, in addition to the Na-borates, found at Searles lake include halite (NaCl), trona (Na2CO3.NaHCO3.2H2O), nahcolite (NaHCO3), Aragonite/calcite (CaCO3), and dolomite (CaMg(CO3)2), in addition to many others (Eugster and Smith, 1965).

Borax, tincalconite, and kernite are among the most common Na-borates found in economic borate deposits. Borates are common constituents of evaporite deposits in regions with a history of volcanism or hydrothermal activity (Woods, 1994). Evaporitic borate deposits occur in many countries throughout the world. The largest volume producers of borates are the United States, Turkey, Russia, Kazakhstan, Peru, China, Chile, Bolivia, Argentina (Warren, 2006). The US and Turkey provide 50% of the borates in the world on a product ton basis (Warren, 2006). Some of the most significant Na-borate deposits are found in California (USA), Argentina, and Turkey. Schaller (1936) discusses the Kramer Na-borate deposit as having been the replacement of Ca-borates and Na-Ca borates. Warren (2006) reported that the mineral zonation seen in many

of the borate deposits around the world were previously thought to be a diagenetic overprint (Inan et al.,1973), like that described by Schaller (1936). Later studies have shown that some of these deposits are fractionated by hydrologically controlled separation of evaporite minerals and reflect subsidence and climate (i.e. layering) (Warren, 2006 and Helvaci and Orti, 2004).

Geologic and experimental observations generally indicate that borax is the first Na-borate mineral to form in evaporite deposits (in the $Na_2B_4O_7$-$H_2O$ system), and later converts into tincalconite and/ or kernite (Christ and Garrels, 1959). Tincalconite appears to be the first dehydration product from borax, forming readily at ambient surface temperatures when borax is exposed to air. When tincalconite is exposed to higher humidity, it returns to the borax phase (Christ and Garrels, 1959). The reversibility of the borax to tincalconite transitions appear to be dependent on humidity and temperature. At low temperatures, borax dehydrates either to an amorphous phase (Christ and Garrels, 1959) or converts to tincalconite. The less hydrous and denser kernite becomes stable at elevated temperatures (Smith and Medrano, 1996). Kernite occurs at greater depths in evaporite deposits, and appears to form through thermal diagenesis of borax (Christ and Garrels, 1959). Field relations suggest that direct conversion of borax to kernite occurs at 331 ± 5 K and at a depth of 760 ± 150 m in the Boron deposit, California, without formation of tincalconite (Christ and Garrels, 1959). Formation of kernite in the lab from borax or aqueous solutions has been successful only above 365 K (Christ and Garrels, 1959; Kemp, 1956). Kernite crystals grow slowly in laboratory conditions, indicating that kinetic factors may in part explain the discrepancy between geologic and laboratory observations of this paragenesis (Smith and Medrano, 1996).

Tincalconite has been found as a primary mineral at Searles Lake, California (Pabst and Sawyer, 1957, and Bowser, 1965). They reported that tincalconite crystals formed directly from

solution, instead of psuedomorphing borax, as seen at the Kramer Deposit (in the pure $Na_2B_4O_7{\cdot}H_2O$ system) (Christ and Garrels, 1959). Pabst and Sawyer (1957) attribute the formation of primary tincalconite to the presence of other ions, such as $Na^+$, $Cl^-$, $SO_4^-$.

The relative stabilities of borax, tincalconite, and kernite can be described through chemical equations relating their stability in the presence of liquid or gaseous water:

$$Na_2B_4O_5(OH)_4 \cdot 8H_2O \Leftrightarrow Na_2B_4O_5(OH)_4 \cdot 2.6H_2O + 5.333H_2O \qquad (1\text{-}1)$$

borax tincalconite

$$Na_2B_4O_5(OH)_4 \cdot 8H_2O \Leftrightarrow Na_2B_4O_6(OH)_2 \cdot 3H_2O + 6H_2O \qquad (1\text{-}2)$$

borax kernite

and

$$Na_2B_4O_5(OH)_4 \cdot 2.6H_2O \Leftrightarrow Na_2B_4O_6(OH)_2 \cdot 3H_2O + 2H_2O \quad . \qquad (1\text{-}3)$$

tincalconite kernite

Note that the stoichiometry of equations (1-1) and (1-3) are dependent on the stoichiometry of tincalconite, which is –re-assessed in this study. Phase stability of these sequences is intriguing because borax converts rapidly to tincalconite despite the apparent metastablity of the latter (Bowser, 1965). Figure 1-4 summarizes reported phase relations of this suite of sodium borate minerals.

## Questions Addressed in the Present Study

The stability, formation, and phase relations of borax, tincalconite, and kernite are poorly understood. Borax is known to precipitate as a primary phase, but the occurrence of tincalconite as a primary phase is controversial. Most authors consider tincalconite to be a purely metastable phase among 1:2 sodium borates in contrast to reports of its apparent formation as a primary phase. Thus, does tincalconite have a true stability field, and if so, under what conditions (e.g.,

temperature, pressure, relative humidity)? Tincalconite and kernite are often found as pseudomorphs of borax, but what conditions allow mineral transformation to borax? In addition to the questions about tincalconite's stability, its stoichiometry has been debated throughout the literature. Several researchers have attempted to refine the stoichiometry, but which is correct?

A complete set of thermodynamic properties have been measured for borax under standard conditions, which facilitates retrieval of the properties of the other substances from equilibrium observations. However, no experimental observations are available for the heat capacity ($C_p$) as a function of temperature of borax (or the other two minerals) necessary for evaluating properties of reactions at elevated temperature. In addition, there are considerable discrepancies between reported values of the enthalpy and Gibbs energies of formation ($\Delta H_f°$ and $\Delta G_f°$, respectively). Therefore what are the thermodynamic properties of formation and reaction of borax, tincalconite, and kernite? Once the thermodynamic properties of the minerals are determined, they can be utilized to answer some of the questions addresses above, although there may not be enough detail to answer all of them.

The present study addresses the stability and paragenesis of Na-borates through experimental observations and modeling of the stability and thermodynamic properties of borax, tincalconite, and kernite. The thermodynamic properties were determined using a combination of differential scanning calorimetry, hydrofluoric acid calorimetry, X-ray diffraction, and equilibrium observations. The stability of the minerals was addressing using new experimental techniques, such as the dual TGA-DSC (Neuhoff and Wang, 2007b) and equilibrium experiments. Experimental observations were synthesized through thermodynamic modeling to assess the stability of each phase as a function of temperature, pressure, and system composition in order to constrain geochemical processes in B-rich systems at Earth's surface. Due to the

similarities in the structure and behavior, these findings can be applied to other borate systems, like the Ca, Na-Ca, and Mg- borates.

Table 1-1. The mineral phases, stoichiometries, and crystal structures of 1:2 Na:B borate minerals. (Burns et al. 1995)

| Mineral Phase | Stoichiometry | Crystal Structure |
|---|---|---|
| Borax | $Na_2B_4O_5(OH)_4 \cdot 8H_2O$ | 2 $B\Phi_3$ triangular complexes and 2 $B\Phi_4$ tetrahedrons |
| Tincalconite | $Na_2B_4O_5(OH)_4 \cdot 2.667H_2O$ | 2 $B\Phi_3$ triangular complexes and 2 $B\Phi_4$ tetrahedrons |
| Kernite | $Na_2B_4O_6(OH)_2 \cdot 3H_2O$ | 3 $B\Phi_3$ triangular complexes and 4 $B\Phi_4$ tetrahedrons; 3 of the above 2 with one borate polyhedral connection |

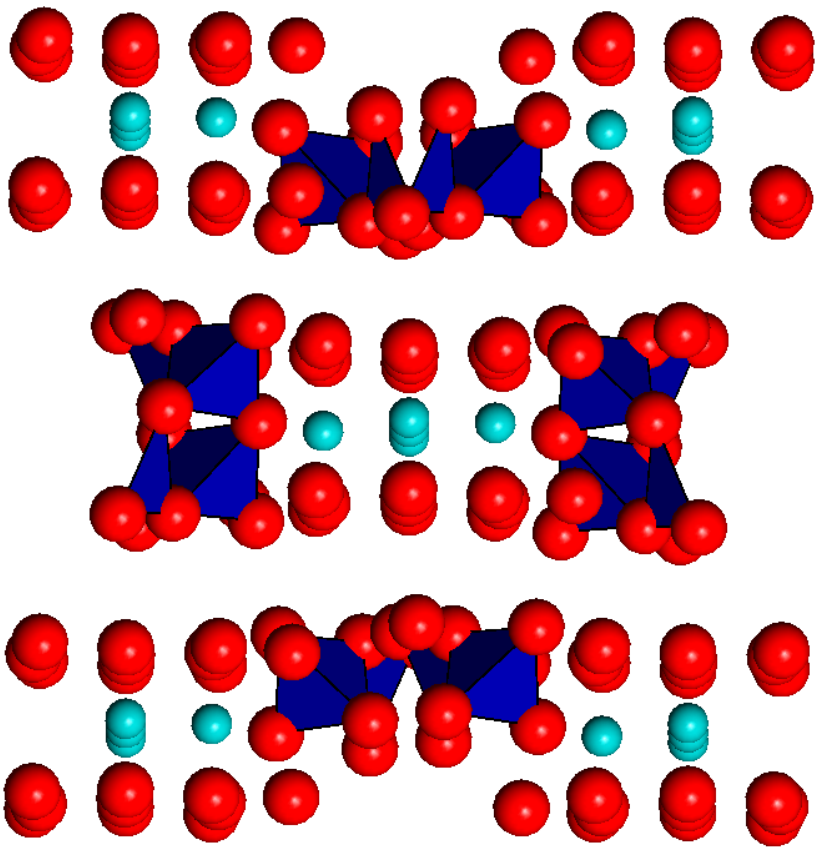

Figure 1-1. Borax borate structure looking down the C axis. The green spheres represent sodium, the blue polyhedra are boron, and the red spheres are oxygen. Borax is made up of two borate triangles and two borate tetrahedrals. (Figure drafted in XtalDraw (Downs, 2005) using atomic coordinates reported by Levy and Lisensky, 1978)

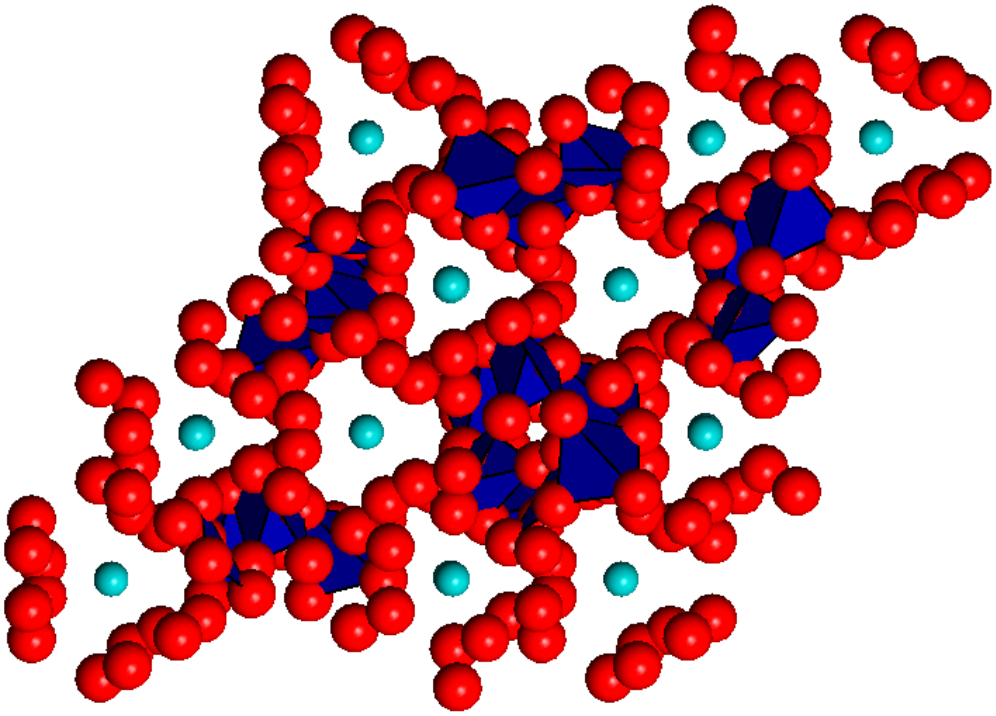

Figure 1-2. Tincalconite borate structure looking down the C axis. The green spheres represent sodium, the blue polyhedra are boron, and the red spheres are oxygen. Tincalconite is made up of two borate triangles and two borate tetrahedrals. (Figure drafted in XtalDraw (Downs, 2005) using atomic coordinates reported by Luck and Wang, 2002)

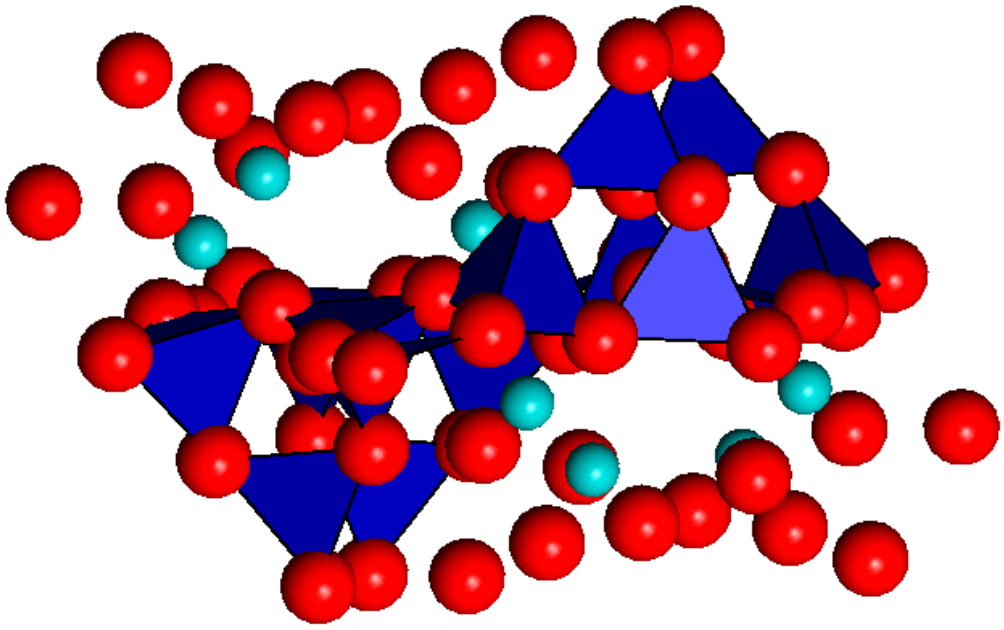

Figure 1-3. Kernite borate structure looking down the C axis. The green spheres represent sodium, the blue polyhedra are boron, and the red spheres are oxygen. Kernite is made up of three borate triangles and four borate tetrahedrals. (Figure drafted in XtalDraw (Downs, 2005) using atomic coordinates reported by Cooper et al., 1973)

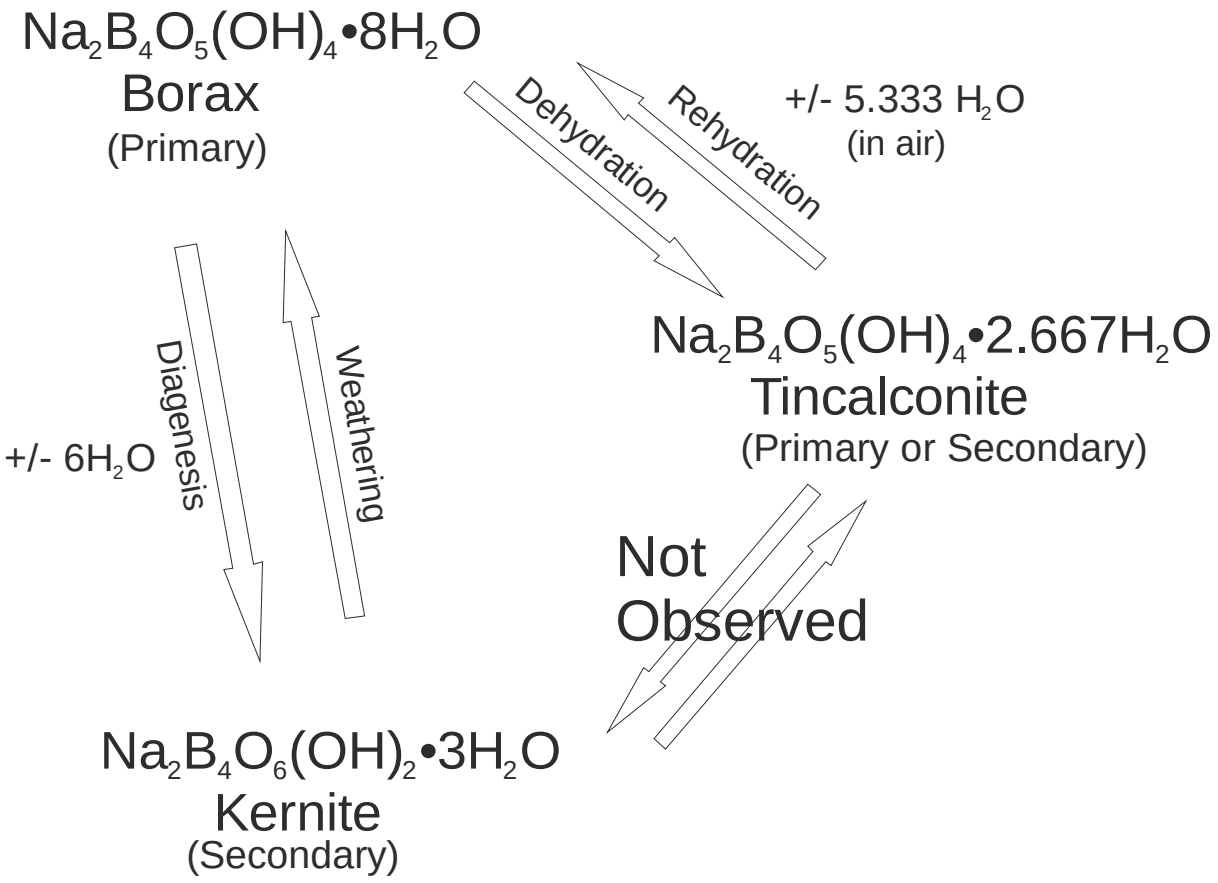


Figure 1-4. Paragenetic relationships between borax, tincalconite, and kernite. The reaction from borax to tincalconite involves a loss of 5.333 water molecules (per Na2) and is common during surficial diagenesis under relatively dry conditions. Tincalconite can reconvert to borax by gaining 5.333 water molecules to become borax. The reaction from borax to kernite involves 6 water molecules, with borax undergoing thermal diagenesis to the less-hydrous phase kernite. Kernite can reconvert under humid conditions to borax. Direct reaction between tincalconite and kernite has not been observed.

# CHAPTER 2
# METHODS

## Samples and Characterization

The experiments described below were conducted on phase pure samples of borax, tincalconite, and kernite. Synthetic ultrapure (>99%) borax (sodium tetraborate decahydrate; Fisher Chemical) was used in the experiments and as a starting material for the preparation of tincalconite. Tincalconite was synthesized by dehydrating synthetic borax in a desiccator containing a saturated solution of LiCl (11.30% RH) at room temperature (298.15 K) for one month. Natural kernite from Boron, CA (USA) was used in the experiments. Phase pure kernite was obtained by lightly crushing a large crystal fragment and hand-picked under a binocular microscope. Although the chemical composition of the kernite sample used in this study was not determined directly due to difficulties in quantifying B contents, it is assumed that this sample is stoichiometric as are all previously reported analyses from Boron, CA and other localities (Hurlbut et al., 1973). All samples were hand ground in an agate mortar. Sample purity was assessed by X-ray powder diffraction (XRPD) using CuK-α at 45 kV, and 30 mA, with typical scans covering 5-50º 2Θ. Water contents were measured by thermogravimetric analysis (TGA) by scanning heating in dry $N_2$ at heating rates of 15 K/min from 298 to 973K on a Netzsch STA 449C Jupiter simultaneous differential scanning calorimeter-thermogravimetric analysis (DSC-TGA) apparatus.

## Equilibrium Experiments

Phase relations between borax and tincalconite were determined as a function of temperature and relative humidity using a modified version of the salt buffer methods described by Chou et al. (2002). Samples of borax and tincalconite (~0.2- 0.4g) were placed in pre-weighed 0.5 ml Eppendorf tubes. The open Eppendorf tubes were then set in shell vials within

scintillation vials containing various buffer salt solutions of known relative humidity (RH) ranging from ~ 5 to ~97% (saturated solutions of $K_2SO_4$, KCl, NaCl, $NaNO_3$, NaI, LiI, LiBr, LiCl, KI, $CoCl_2$, $MgNO_3$, and $MgCl_2$; Greenspan, 1977; or NaCl solutions of fixed molality; Cherife and Resnik, 1984). The borax and tincalconite samples were reacted at 298.15 K, 313.15 K, 328.15 K, and 338.15 K for ~ 4 days, except for those at 298.15 K which were allowed to equilibrate for 4 weeks. Temperature was controlled by submerging the scintillation vials in a constant temperature water bath except those at 298.15 K which were placed in a climate controlled laboratory. Reaction progress was assessed by monitoring mass changes of individual samples and phase identities of experimental products determined by XRPD.

## Calorimetry

Heats of solution in HF of borax, tincalconite, and kernite were measured at Lafayette College using a calorimetric system described by Hovis and Roux (1993) and Hovis et al. (1998). Samples (~200 mg) were dissolved in 910.1 g (~ 1 L) of 20.1 wt % hydrofluoric acid (HF) at 323.15 K under isoperibolic conditions utilizing an internal sample container (Waldbaum and Robie 1970). Experiments were run in duplicate.

Heat capacities of borax, tincalconite, and kernite and the heat of dehydration of borax to tincalconite were measured by DSC on a Netzsch STA 449C Jupiter simultaneous DSC-TGA apparatus. Gas flow (ultrapure $N_2$) was maintained at ~30 mL/min using mass-flow controllers. A multipoint temperature calibration curve was developed using the melting points of $H_2O$, Ga, In, Sn, Bi, Zn, and Al along with the solid-solid transition points of cesium chloride and quartz (Cammenga et al. 1993, Gmelin and Sarge 2000; Höhne et al. 1990; Sabbah et al. 1999, Price 1995). Due to the incompatibility of many of these materials with the Pt-Rh crucible used in the experiments, temperature calibration was conducted in identical crucibles lined with a sub-mm think insert of alumina. Caloric calibration was accomplished using the DSC response of

synthetic sapphire (Gmelin and Sarge 2000; Sabbah et al. 1999; Sarge et al. 1994; Stølen et al. 1996). All experiments were conducted in Pt-Rh crucibles with unsealed, perforated lids using sample masses between 20 and 30 mg.

Heat capacity measurements were conducted from 273 to 315 K. Samples were run in duplicate with each experiment consisting of four separate runs: (1) a background correction with an empty crucible; (2) a single-crystal sapphire caloric background; (3) the mineral sample; and (4) repeat of the background correction. Standard response was compared between experiments to test for reproducibility. Companion experiments on quartz yielded Cp measurements within 1% of previously reported values.

The enthalpy of dehydration of borax to tincalconite was measured at 348 K using a modified version of the technique described by Neuhoff and Wang (2007b) Measurements were made at a heating rate of 15 K per min by scanning DSC measurements made on a Netzsch STA 449C Jupiter simultaneous DSC-TGA apparatus. Ultrapure $N_2$ was used for the experiments. Each sample of borax was kept over a saturated $K_2SO_4$ solution until transfer to the crucible in order to prevent dehydration. For each run, 20-30mg of borax was heated rapidly (15 K.min) from room temperature to 348 K under ultrapure $N_2$. Temperature was held constant for a period of 2 hours to allow the sample to dehydrate. Reaction progress and heat effects were monitored by continuous application of the DSC and TGA signals. Calculations of the heats of dehydration were performed based on correlations between the DSC and TGA signals following the methods of Neuhoff and Wang (2007b).

# CHAPTER 3
# RESULTS

## Thermal Analysis

Thermogravimetric analysis and differential scanning calorimetric observations of borax, tincalconite, and kernite are shown in Figure 3-1. Borax exhibits three distinct dehydration events, as evidenced by the three endothermic peaks in the DSC curve. This initial mass loss corresponds to a dehydration event evidenced by the endothermic peak centered at 365 K. A second mass loss and dehydration event occurs at 391 K corresponding to a 25% mass loss. The third dehydration event occurred at 434 K with a mass loss of 22%. Comparison with the results for tincalconite discussed below indicates that the first two dehydration events correspond to the transition from borax to tincalconite. The third dehydration event results in complete loss of water from borax to form anhydrous $Na_2B_4O_7$ phase. The total mass loss to 975 K was 47%, in good agreement with the expected 47.24% loss expected from the stoichiometric amounts of molecular water and hydroxyl groups in the formula.

Tincalconite exhibited one distinct dehydration event. The dehydration event occurred at 434 K with a mass loss of ~29%. This matched the expected mass loss from release of its water molecules (Luck and Wang, 2002, and Pabst and Sawyer, 1998). At 918 K an exothermic peak in the DSC curve is present that does not correlate with any mass change. This peak may represent amorphization of the sample. Outside of this exothermic peak, the tincalconite TGA and DSC curves replicate the latter portion of the borax curves. After the borax loses the initial 25% mass (its first two dehydration events), the TGA curve mimics the gradual mass loss shown in the tincalconite curve. The tincalconite DSC curve also matches the third dehydration event in borax, consistent with initial transformation of borax into tincalconite followed by complete dehydration of a tincalconite phase in the borax experiments.

Although the stoichiometry of tincalconite has traditionally been given as $Na_2B_4O_5(OH)_4 \cdot 3H_2O$ (Muessig and Allen, 1957), recent X-ray diffraction results suggest that the stoichiometric tincalconite is somewhat less hydrous. Based on water site occupancies determined through single crystal diffraction, Luck and Wang (2002) suggested that the composition of tincalconite corresponds to $Na_2B_4O_5(OH)_4 \cdot 2.667H_2O$. In the experiments shown in Figure 3-1, the initial two dehydration events (which are not observed in tincalconite) correspond to a mass loss of ~25.5%. Given molecular weights for borax and tincalconite of 381.36g/mol and 285.28g/mol, respectively (based on the formula unit proposed by Luck and Wang, 2002), the corresponding mass loss during the transition between these two phases should be 25.2%. This is consistent with the observations shown in Figure 3-1. In contrast, if the more hydrous stoichiometry of tincalconite were correct, the resulting mass loss would amount to only 23.5%. The discrepancy between this prediction and the experimental results shown in Figure 3-1 is larger than the likely error in the experimental results (~0.1% of the mass change).

Kernite exhibits two distinct dehydration events, followed by a gradual loss of water resulting in a total mass loss of 26.4%. The initial mass loss corresponds to ~10% of the initial mass related to an endothermic reaction at 438 K. The second dehydration event occurred at 469 K with an additional 7% mass loss. The mass continues to decrease with temperature, finally leveling off at a 26.4% loss. The expected total mass loss from the dehydration of kernite is 26.1% (Hurlbut, 1973).

## Equilibrium Observations

Figure 3-2 shows the results of an experiment run at 298.15 K left to equilibrate over 4 weeks. Borax (open circles) did not lose any mass above an RH of 53%, below which mass loss signaled the dehydration to tincalconite. The mass of borax decreased systematically with decreasing humidity down to 18% RH, at which point the mass loss was 25.5% corresponding to

complete transformation to tincalconite. The tincalconite samples (dark circles) exhibited no mass change at RH values below 65%; above this humidity, tincalconite began to absorb water and gained mass as it converted to borax. The mass of tincalconite systematically increased with increasing relative humidity until 84% RH, at which point the mass gain was ~33% signaling the complete transition to borax. (The percentage increase in hydration is greater than the percent decrease because of the smaller mass at commencement in hydration reaction). As discussed below, the progressive decrease in the mass of borax with decreasing humidity and increase in the mass of tincalconite with increasing humidity reflects incomplete conversion due to kinetic limitations that depend on the driving force of the reaction (humidity) and do not reflect solid solution between these phases. Thus at 298.15 K equilibrium between borax and tincalconite occurred at 59 +/- 6% relative humidity.

Figure 3-3 shows the results of XRPD characterization of borax, tincalconite, and a sample of intermediate composition labeled "sample X" (borax sample that lost ~12.12% of mass) formed by partially dehydrating borax at 313.15 K and 48.42% relative humidity for 4 days. Sample X is analogous to the samples in Figure 3-2 that exhibited an intermediate mass loss (i.e. not entirely transformed to borax or tincalconite). Phase pure borax and tincalconite are clearly distinguished with unique peaks for borax, 14.88º, 15.54º, and 18.32º 2Θ, while tincalconite peaks occur at 10.06º, 18.84º, and 20.24º 2Θ. The borax and tincalconite peaks are all present in the pattern of sample X. No additional peaks are observed in the pattern of sample X. This suggests that sample X is a mechanical mixture of borax and tincalconite rather than being a solid solution of these phases (which would be evidenced by shifting peak positions and/or identities).

The results of the experiments as a function of temperature and relative humidity are summarized in Figure 3-4 and Table 3-1. The black line in Figure 3-4 represents equilibrium between borax and tincalconite calculated from the thermodynamic model described in Chapter 4. Also shown for comparison are previous observations of equilibrium between these two phases. It can be seen in Figure 3-4 and Table 3-1 that the RH at equilibrium between borax and tincalconite increases steadily from 59 ± 6% RH at 298.15 K to 84.5 ± 4.5% RH at 328.15 K. Borax was not stable at 338.15 K with tincalconite stable up to 80% RH and borax transformation to tincalconite over this range of RH as well. At 338.15 K and 97% RH both samples deliquesced as evidenced by the formation of an aqueous solution on the sample and an increase in mass above that of borax. Deliquesence under these conditions indicates that a sodium tetraborate-saturated solution has an equilibrium vapor pressure lower than 97% at 338.15 K. Each phase reported was confirmed by XRPD.

## Heat Capacity

The measured heat capacities ($C_p$) of borax, tincalconite, and kernite are listed in Table 3-2 and plotted as a function of temperature in Figure 3-5. It can be seen in Figure 3-5 that $C_p$ increases monotonically for each mineral over the temperature range shown, indicating that no phase transitions or dehydration events occurred during the heat capacity measurements.

## Calorimetric Observations of Heats of Hydration

Table 3-3 shows the measurements from the HF calorimetric experiments. The average enthalpy of solution ($\Delta H^{o}_{(sol)}$) for borax, tincalconite, and kernite, as well as errors taken to be twice the standard deviation of the individual experimental results, are shown as well. The error associated with borax, tincalconite, and kernite is 0.1%, 0.7%, and 0.5% of the total heat of solution, respectively.

The results given in Table 3-3, along with the previously determined $\Delta H^{o}_{sol}$ for liquid water (G. Hovis, pers. communication), were used to calculate the enthalpies of dehydration reactions 1-1 through 1-3 using the thermochemical cycles shown in Table 3-4. The resulting $\Delta H_R$ for reactions 1-1 through 1-3 at 323.15 K are shown in Table 3-5. Using the heat capacity measurements described above, the $\Delta H_R$ at 298.15 K was calculated from the relation

$$\Delta H_{R,323.15K} = \Delta H_{R,298.15K} + \int_{298.15}^{323.15} C_{p,substance} dT \qquad (3\text{-}1)$$

and is also listed in Table 3-5.

Evaluation of $\Delta H_R$ for reaction (8) was determined directly from simultaneous DSC-TGA measurements following the methods of Neuhoff and Wang (2007b). Due to lack of a suitable background, $\Delta H_R$ was calculated from a linear regression of the DSC signal and the first derivative of the TGA signal (dTGA; cf. Neuhoff and Wang, 2007b) via the equation

$$\Delta H^{o}_{R,T,P} = kA(\Delta m)^{-1} (MW_{H2O}) \qquad (3\text{-}2)$$

where $A$ is the area of the DSC peak (in μVs), k is the calibration factor (in W/μV), $\Delta m$ is the mass change measured by TGA, and $MW_{H2O}$ is the molecular weight of water. Over the range of mass change expected for the borax to tincalconite transition, the DSC and dTGA signals were linearly correlated indicating that the nature of the reaction was constant over the whole range of reaction progress. This observation helped confirm findings between individual experiments as well, despite visible differences in the shape of the DSC and dTGA peaks between experiments. The enthalpy of reaction at 323.15 K calculated from these experiments (taking into account the enthalpy of vaporization of water from Wagner andPruß, 2002) is given in Table 3-5 along with that evaluated via equation 8 at 298.15 K. It can be seen in Table 3-5 that $\Delta H_R$ determined through HF calorimetry and by DSC agree within error.

Table 3-1. Equilibrium experiment results showing the range of relative humidity at which the borax to/from tincalconite reaction takes place.

| Temperature (K) | Maximum RH for Tincalconite Stability (%) | Minimum RH for Borax Stability (%) |
|---|---|---|
| 298.15 | 52.98 | 64.92 |
| 313.15 | 71.00 | 74.68 |
| 328.15 | 80.70 | 89.19 |
| 338.15 | 79.85 | NA |

Table 3-2. Heat Capacities of borax, tincalconite, and kernite were measured by differential scanning calorimetry.

| | | Cp (J/molK) | |
|---|---|---|---|
| Temperature (K) | Borax | Tincalconite | Kernite |
| 253.15 | | 308.8 | |
| 255.15 | | 311.0 | |
| 257.15 | | 313.3 | |
| 259.15 | | 315.7 | |
| 261.15 | | 318.1 | |
| 263.15 | | 320.6 | |
| 265.15 | | 323.0 | |
| 267.15 | | 325.5 | |
| 269.15 | | 327.8 | |
| 271.15 | | 330.3 | |
| 273.15 | 535.2 | 332.8 | 313.4 |
| 275.15 | 539.6 | 335.4 | 315.4 |
| 277.15 | 544.3 | 337.2 | 317.5 |
| 279.15 | 548.3 | 339.8 | 319.3 |
| 281.15 | 552.5 | 342.3 | 321.3 |
| 283.15 | 556.7 | 344.9 | 323.4 |
| 285.15 | 560.6 | 347.3 | 325.2 |
| 287.15 | 564.5 | 349.7 | 327.0 |
| 289.15 | 568.6 | 352.2 | 329.0 |
| 291.15 | 572.6 | 354.6 | 330.8 |
| 293.15 | 576.5 | 357.1 | 332.7 |
| 295.15 | 580.5 | 359.8 | 334.6 |
| 297.15 | 584.5 | 362.4 | 336.4 |
| 299.15 | 588.6 | 365.2 | 338.3 |
| 301.15 | 592.5 | 367.8 | 340.0 |
| 303.15 | 597.0 | 370.7 | 342.0 |
| 305.15 | 601.4 | 373.6 | 343.9 |
| 307.15 | 606.2 | 376.6 | 345.9 |
| 309.15 | 611.0 | 379.7 | 347.9 |
| 311.15 | 616.4 | 383.1 | 350.2 |
| 313.15 | 622.4 | 386.7 | 352.6 |
| 315.15 | | | 355.4 |

Table 3-3. Measurements made during the HF experiments.

| Sample | Assumed composition | Formula Weight (g/mol) | Sample Weight (g) | Temperature change during dissolution (°C) | Mean Solution temperature (°C) | Calorimeter Cp before dissolution (J/deg) | Calorimeter Cp after dissolution (J/deg) | Enthalpy of solution from Cp before dissolution (kJ/mol) | Enthalpy of solution from Cp after dissolution (kJ/mol) | Average Enthalpy of Solution | Standard Deviation |
|---|---|---|---|---|---|---|---|---|---|---|---|
| Borax | $Na_2B_4O_7.10H_2O$ | 381.37 | 0.26 | 0.046 | 49.876 | 3866.3 | 3866.1 | -256.83 | -256.82 | | |
| Borax* | $Na_2B_4O_7.10H_2O$ | 381.37 | 0.25 | 0.044 | 49.892 | 3874.5 | 3872.4 | -256.70 | -256.56 | -256.73 | 0.255 |
| Tincalconite | $Na_2B_4O_5(OH)_4.2.6667H_2O$ | 285.29 | 0.25 | 0.071 | 49.933 | 3871.0 | 3871.1 | -311.10 | -311.10 | | |
| Tincalconite* | $Na_2B_4O_5(OH)_4.2.6667H_2O$ | 285.29 | 0.25 | 0.071 | 49.935 | 3870.3 | 3869.6 | -312.16 | -312.10 | -311.61 | 1.191 |
| Kernite | $Na_2B_4O_6(OH)_2\text{-}3H_2O$ | 273.28 | 0.20 | 0.059 | 49.920 | 3866.4 | 3865.3 | -313.27 | -313.18 | | |
| Kernite* | $Na_2B_4O_6(OH)_2\text{-}3H_2O$ | 273.28 | 0.20 | 0.060 | 49.932 | 3864.2 | 3864.3 | -313.94 | -313.95 | -313.59 | 0.832 |

* Dissolved in acid of the preceding experiment.

Table 3-4. Thermochemical cycles employed in the calculation of enthalpy of reaction.

| Equation number | Reaction | $\Delta H^\circ_R$ (kJ/mol) |
|---|---|---|
| 1 | Borax + HF = Solution 1 | $=\Delta H^\circ_{Sol(Borax)}$ |
| 2 | Tincalconite + HF = Solution 2 | $=\Delta H^\circ_{Sol(Tincalconite)}$ |
| 3 | $H_2O$ + HF = Solution 3 | $=\Delta H^\circ_{Sol(Water)}$ |
| 4 (Reaction 1-1) | Borax = Tincalconite + $5.333H_2O$ | $=\Delta H^\circ_{Sol(Borax)} - \Delta H^\circ_{Sol(Tincalconite)} - 5.333\Delta H^\circ_{Sol(Water)}$ |
| 5 | Kernite + HF = Solution 4 | $=\Delta H^\circ_{Sol(Kernite)}$ |
| 6 (Reaction 1-2) | Borax = Kernite + $6H_2O$ | $=\Delta H^\circ_{Sol(Borax)} - \Delta H^\circ_{Sol(Kernite)} - 6\Delta H^\circ_{Sol(Water)}$ |
| 7 (Reaction 1-3) | Tincalconite= 3Kernite + $2H_2O$ | $=\Delta H^\circ_{Sol(Tincalconite)} - \Delta H^\circ_{Sol(Kernite)} - 5.333\Delta H^\circ_{Sol(Water)}$ |

Table 3-5. $\Delta H_R$ calculated from HF calorimetric measurements and DSC calorimetric measurements.

| Reactions (Table 3-4) | $\Delta H_R$ (kJ/mol) | | | |
|---|---|---|---|---|
| | 298.15K (HF Method) | 323.15K (HF Method) | 298.15K (DSC Method) | 323.15K (DSC Method) |
| 1-1 | -50.62 ± 1.22 | -54.83 ±1.22 | -51.4 ±1.1 | -55.6 ± 1.1 |
| 1-2 | -52.10 ± 1.45 | -56.80 ± 1.45 | | |
| 1-3 | 2.49 ± 0.87 | -1.96 ± 0.87 | | |

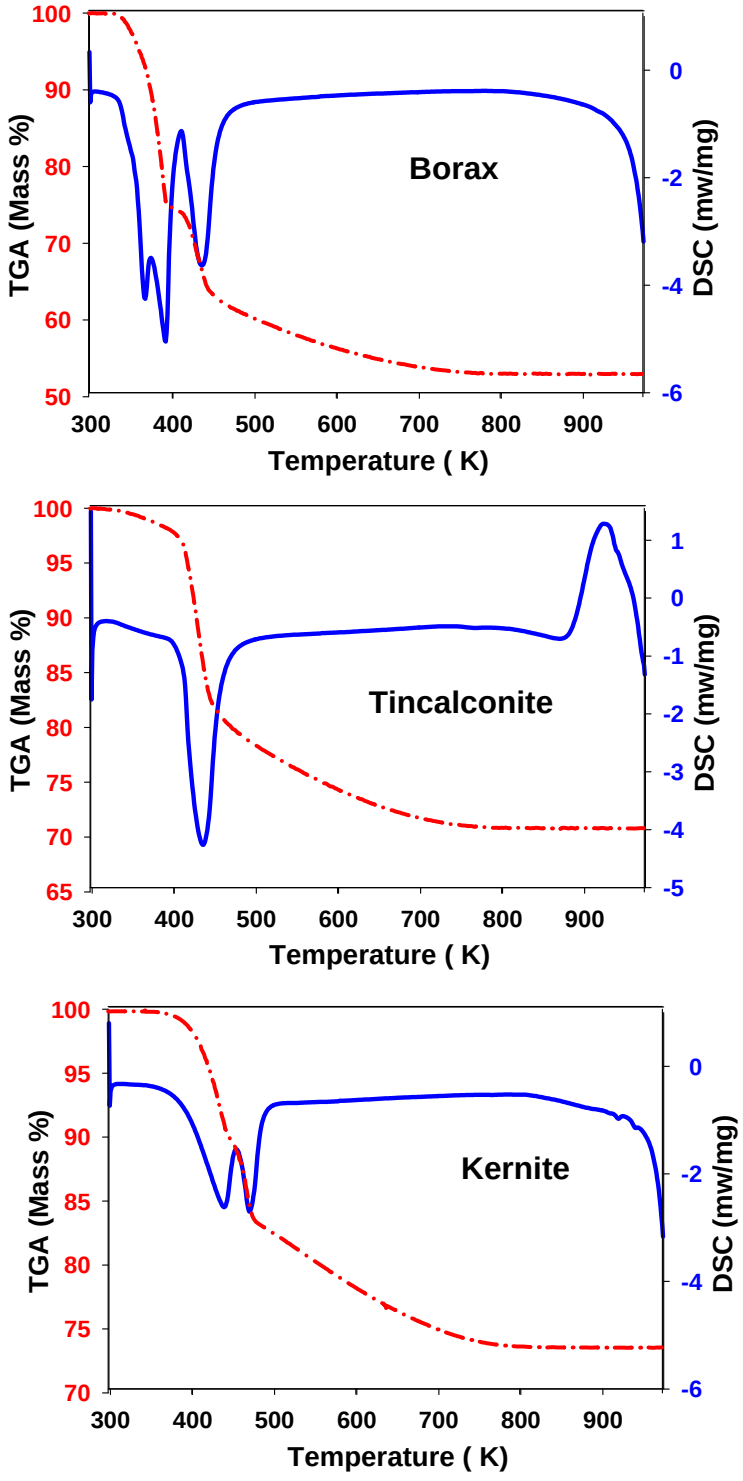


Figure 3-1. Thermal analyses of borax, tincalconite, and kernite (heated from 298K to 973K at 1bar at 15K/min). TGA is shown with the red dotted line and DSC with the blue solid line.

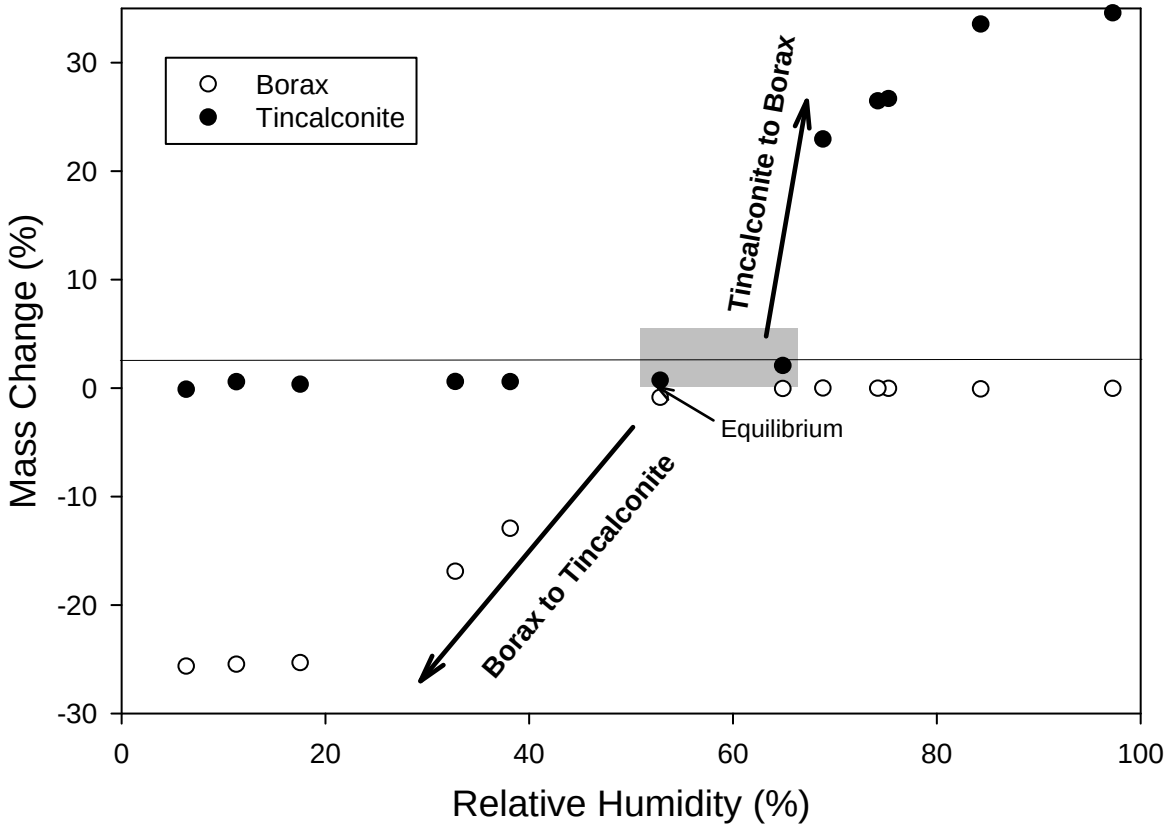


Figure 3-2. Experimental observations of borax and tincalconite reaction at 298.15K. The mass of borax remains constant down to a relative humidity of 53%, then systematically decreases with the RH, eventually completing the transition to tincalconite (25% mass loss) at the RH 18%. The mass of tincalconite remains constant up to a RH of 65% and increases with the relative humidity until it becomes borax at RH 84%.

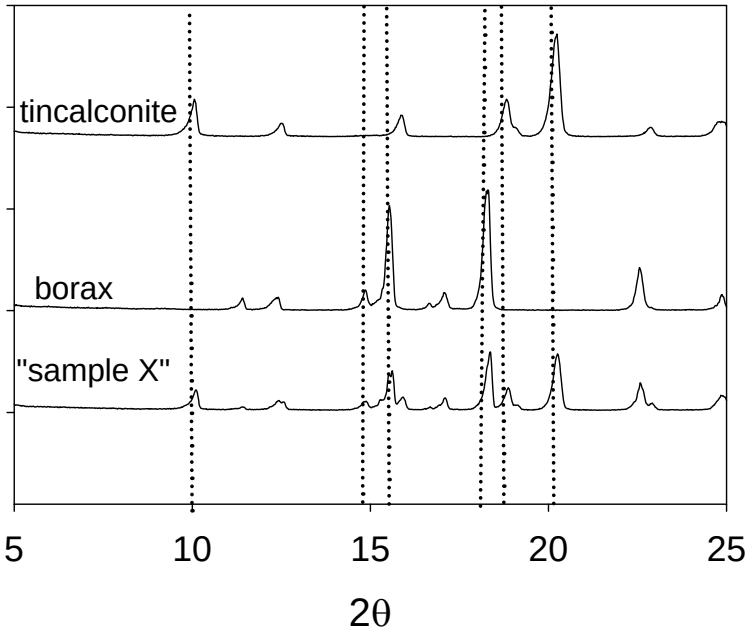


Figure 3-3. X-ray powder diffractograms of phase pure borax, tincalconite, and an intermediate sample formed by partially dehydrating borax at 313.15K and 48.42% relative humidity for 4 days. The dashed lines indicate the positions of characteristic reflections for borax and tincalconite; the diffraction peaks for sample X occur at the same positions. All of the reflections exhibited by sample X correspond to peaks for either borax or tincalconite.

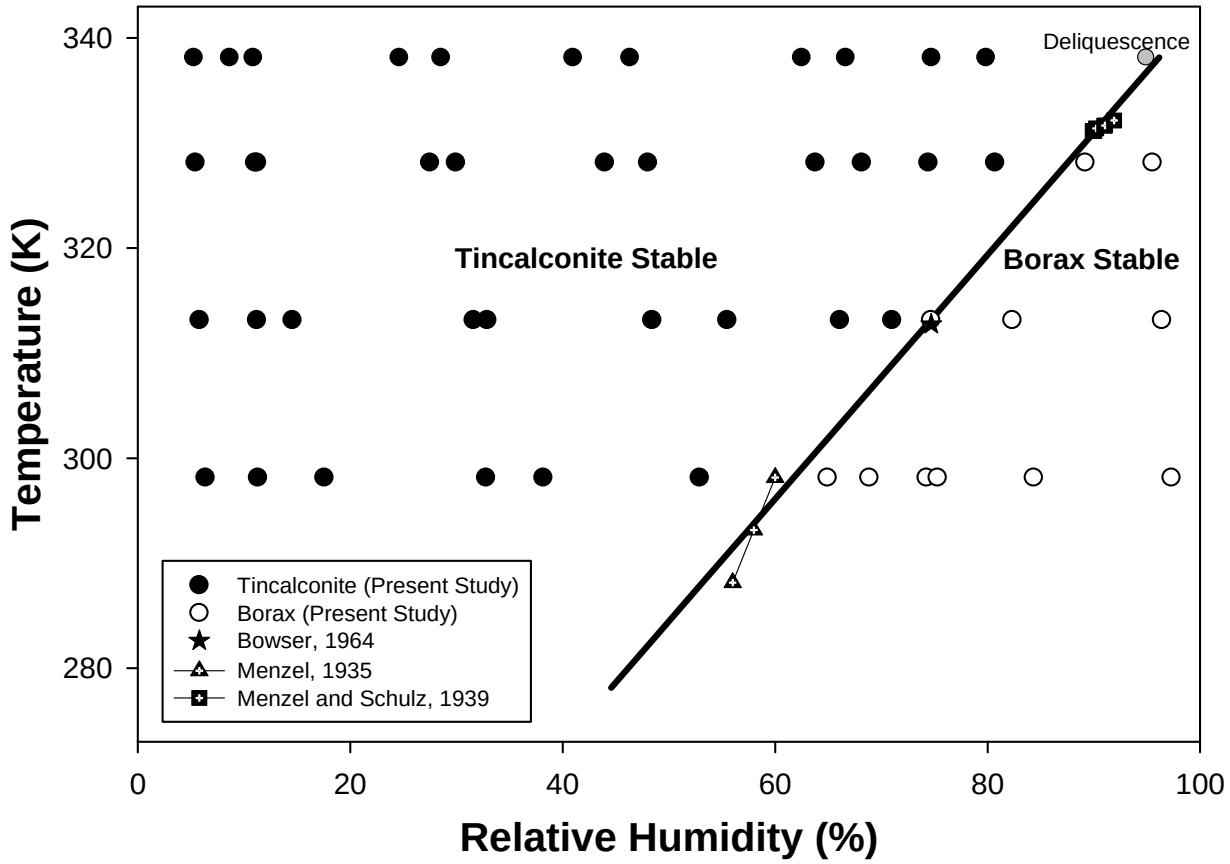


Figure 3-4. Experimental observations of borax and tincalconite stability as a function of temperature and RH. Shown for comparison are observations of RH in equilibrium with borax and tincalconite from Menzel (1935), Menzel and Shulz (1940), and Bowser (1965). The gray symbol denotes conditions under which sodium tetraborate deliquesces. The black curve shows the calculated equilibrium RH as a function of temperature derived in this study.

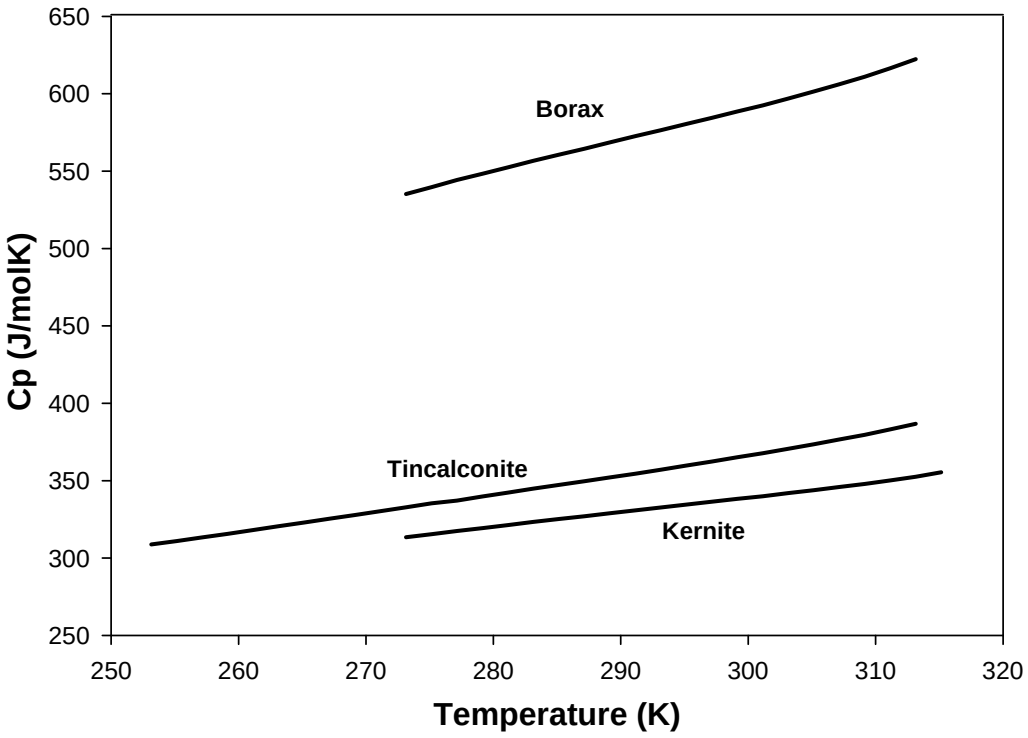


Figure 3-5. Heat capacities of borax, tincalconite, and kernite measured by differential scanning calorimetry.

# CHAPTER 4
# THERMODYAMIC MODEL AND PROPERTIES

The equilibrium constants (*K*) for reactions 1-1, 1-2, and 1-3, respectively, are given by

$$K_{1-1} = \frac{\left[\alpha_{tincalconite}\right]\left[\alpha_{H_2O}\right]^{5.333}}{\left[\alpha_{borax}\right]^3} \tag{4-1}$$

$$K_{1-2} = \frac{\left[\alpha_{\mathrm{ker}\,nite}\right]\left[\alpha_{H_2O}\right]^6}{\left[\alpha_{borax}\right]} \tag{4-2}$$

$$K_{1-3} = \frac{\left[\alpha_{\mathrm{ker}\,nite}\right]^3\left[\alpha_{H_2O}\right]^2}{\left[\alpha_{tincalconite}\right]} \tag{4-3}$$

where $\alpha_X$ is activity of phase *X*. The standard Gibbs energy of reaction ($\Delta G^\circ_{r,T,P}$) is related to the K at *T*, *P* by

$$\Delta G^\circ_{r,T,P} = -RT \ln K_{T,P} \tag{4-4}$$

where R is the gas constant.

The standard enthalpy and entropy of reaction ($\Delta H^\circ_{r,T,P}$ and $\Delta S^\circ_{r,T,P}$, respectively) are related to $\Delta G^\circ_{r,T,P}$ by

$$\Delta G^\circ_{r,T,P} = \Delta H^\circ_{r,T,P} - T\Delta S^\circ_{r,T,P} \quad . \tag{4-5}$$

The change in a thermodynamic property across a reaction at T and P, $\Delta\Xi^\circ_{r,T,P}$ is given by

$$\Delta\Xi^\circ_{r,T,P} = \sum_j \nu_j \Delta\Xi^\circ_{T,P} \tag{4-6}$$

where the summation is over all species j, $\nu_j$ is the stochiometric reaction coefficient for species j, and $\Delta\Xi^\circ_{T,P}$ is the corresponding property of the substance. The Gibbs energy of reaction at T, P is related to the standard molal Gibbs energy of formation ($\Delta G^o_f$) at 298.15 K, 1 bar ($T_{ref}$, $P_{ref}$) via

equation (4-6) by noting that the apparent (cf. Benson, 1968; Helgeson et al., 1978) molal Gibbs energy of formation at $T$, $P$ ($\Delta G^{o}_{f,T,P}$) is given by

$$\Delta G^{\circ}_{f,T,P} = \Delta G^{\circ}_{f,T_{ref},P_{ref}} - S^{\circ}_{T_{ref},P\backslash ref}(T - T_{ref}) + \int_{T_{ref}}^{T} C^{\circ}_{P} dT - T\int_{T_{ref}}^{T} C^{\circ}_{P}\, d\ln T + \int_{P_{ref}}^{P} V_{T_{ref}P_{ref}}{}^{\circ} dP \quad (4\text{-}7)$$

where $S_{Tref,Pref}{}^{o}$ and $V_{Tref,Pref}{}^{o}$ are the standard molal entropy and volume at 298.15 K and 1 bar, respectively, and $Cp^{o}$ is the standard molal heat capacity at T, 1 bar.

The thermodynamic properties adopted by Wagman et al. (1982) for borax (except Cp, for which Wagman et al., 1982 did not evaluate the temperature dependence) were adopted as the basis for subsequent evaluation of the thermodynamic properties of tincalconite and kernite from the results of this study (Table 4-1). Previously reported values of $V_{Tref,Pref}{}^{o}$ for tincalconite and kernite were adopted, though were not directly used in derivation of other thermodynamic properties as all relevant calculations are based on observations at 1 bar. The heat capacity values listed in Table 3-2 were used to regress Maier-Kelley (1932) polynomial expressions of the temperature dependence of this property

$$C_p = a + bT - cT^{-2} \quad (4\text{-}8)$$

for evaluation of the $C_p$ integrals in equation (4-7). In converting between $S_{Tref,Pref}{}^{o}$ and entropies of formation in these calculations, $S_{Tref,Pref}{}^{o}$ of the elements reported by Robie and Hemingway (1995) were adopted. The $S_{Tref,Pref}{}^{o}$ value was calculated from equation (4-9)

$$\Delta S_{f,T,P} = S^{\circ}_{T_{ref},P_{ref}} + \int_{T_{ref}}^{T} C_p dT \ln T - \Sigma \nu_i S^{\circ}_{T_{ref},P_{ref}\ elements} \quad (4\text{-}9)$$

, which was then used to determine the $\Delta S_{Tref,Pref}{}^{o}$ using equation (4-10).

$$\Delta S_{f,T_{ref},P_{ref}} = S^{\circ}_{T_{ref},P_{ref}} - \Sigma \nu_i S^{\circ}_{T_{ref},P_{ref}\ elements} \quad (4\text{-}10)$$

The other thermodynamic properties were then retrieved from equation (4-11)

$$\Delta G^{\circ}_{f,T_{ref},P_{ref}} = \Delta H^{\circ}_{f,T_{ref},P_{ref}} - T\Delta S^{\circ}_{f,T_{ref},P_{ref}} \quad (4\text{-}11)$$

by utilizing the value for $\Delta S_{fTref,Pref}$° from equation (4-10) and $\Delta G^{o}_{f,Tref,Pref}$ from equation (4-7).

The thermodynamic properties of the formation of tincalconite were calculated from the measurements from the equilibrium observations and DSC measurements. The equilibrium constant of the borax/tincalconite reaction was determined using equation (4-1) and utilizing the activities from the equilibrium observations. Once the equilibrium constant was known it was used to determine $\Delta G^{\circ}_{r,T,P}$. Then $\Delta H^{\circ}_{r,T,P}$ was determined from the DSC measurements, therefore both $\Delta G^{\circ}_{r,T,P}$ and $\Delta H^{\circ}_{r,T,P}$ were plugged into equation (4-12) to get the $\Delta G^{\circ}_{f,T,P}$ and $\Delta H^{\circ}_{f,T,P}$, respectively.

$$\Delta \Xi_{fTinc} = \Delta \Xi_{R} - 5.333\Delta \Xi_{fH_2O} + \Delta \Xi_{fBorax} \quad (4\text{-}12)$$

with Ξ representing each of the properties (G and H) of tincalconite. Then $\Delta S_{r,T,P}{}^{o}$ and $S_{f,T,P}{}^{o}$ were calculated using equations (4-10) and (4-9) respectively. Finally, $\Delta G^{o}_{f,Tref,Pref}$ and $\Delta H^{o}_{f,Tref,Pref}$ were calculated using equations (4-7) and (4-11) respectively. The error associated with the DSC measurements and equilibrium observations were compounded by summing the squared errors for each variable, then taking the square root, therefore giving the total error of the thermodynamic properties of formation at 298.15K.

The properties of reaction for kernite were calculated in the same method as tincalconite explained above, although the $\Delta H_R$ came from the HF measurements. Properties of kernite were calculated from the calorimetric observations noted above and the values from Christ and Garrels (1959) of kernite-borax-solution equilibrium at 58.5 ºC, 1 bar, with 96.6% equilibrium RH over the saturated solution. The equilibrium constant of the borax/kernnite reaction was determined

using equation (4-2) and the activity from the Blasdale and Slanksy (1939) and Menzel and Schulz (1940) value of 96.6% RH at 331.65K. Once the equilibrium constant was known it was used to determine $\Delta G^{\circ}_{r,T,P}$ (T= 331.65K). Then $\Delta H^{\circ}_{r,T,P}$ was determined from the HF measurements, therefore both $\Delta G^{\circ}_{r,T,P}$ and $\Delta H^{\circ}_{r,T,P}$ were plugged into equation (4-13) to get the $\Delta G^{\circ}_{f,T,P}$ and $\Delta H^{\circ}_{f,T,P}$, respectively,

$$\Delta \Xi_{Kernite} = \Delta \Xi_{R} - 6\Delta \Xi_{H_2O} + \Delta \Xi_{Borax} \qquad (4\text{-}13)$$

with Ξ representing each of the properties (G and H) of kernite. Then $\Delta S_{r,T,P}{}^{o}$ and $S_{f,T,P}{}^{o}$ were calculated using equations (4-10) and (4-9) respectively. Finally, $\Delta G^{o}_{f,Tref,Pref}$ and $\Delta H^{o}_{f,Tref,Pref}$ were calculated using equations (4-7) and (4-11) respectively. The error associated with the HF measurements and calculations were compounded by summing the squared errors for each variable, then taking the square root. Errors on the thermodynamic properties were taken to be twice the standard deviation of the individual experimental results.

Table 4-1. Thermodynamic properties of borax, tincalconite, and kernite derived in this study.

| At 298.15K | Volume ($cm^3$) | $\Delta G^o_{298.15}$ (kJ/mol) | $\Delta H^o_{298.15}$ (kJ/mol) | $\Delta S^o_{298.15}$ (J/molK) |
|---|---|---|---|---|
| Borax | 222.7 ± 0.2[a] | -5516.02[a] | -6288.59[a] | 586.01[a] |
| Tincalconite | 2279.3[b] | -4244.48 ± 8.58[d] | -4713.60 ± 8.58[d] | 360.66 ± 2.83[d] |
| Kernite | 143.54±0.02[c] | -4086.30 ± 8.57[d] | -4580.19 ± 8.57[d] | 337.01 ± 2.67[d] |

[a]-Wagman et al. 1982; [b]- Luck and Wang, 2002; [c]- Cooper et al. 1973; [d]-Present study.

Table 4-2. Maier Kelley Coefficients of borax, tincalconite, and kernite.

| Minerals | a | b | c |
|---|---|---|---|
| Borax | -9.244 | 0.50207 | 0.0 |
| Tincalconite | -3.252 | 0.30318 | 0.0 |
| Kernite | 11.81 | 0.23099 | 0.0 |

# CHAPTER 5
# DISCUSSION

## Comparison with Previous Thermal Analysis Results

The thermal analysis results of this study generally agree well with those of prior observations of the thermal behavior of borax, tincalconite, and kernite. In Figure 3-1, it can be seen that the first endothermic reaction of borax occurred at 93ºC, compared to 90ºC as compared observed by Giese and Kerr (1959) and 74ºC as observed by Waclawska (1998). The second endothermic reaction was observed at 117ºC in this study, as opposed to 130ºC (Giese and Kerr, 1959) and 102ºC (Waclawska, 1998). The third reaction was observed in this study at 161ºC, as opposed to 155ºC (Giese and Kerr, 1959) or 133ºC (Waclawska, 1998). In all three studies, the first two reactions signaled the transition of borax to tincalconite via dehydration. The transition temperatures observed in the present study are systematically higher than observed by Giese and Kerr (1959) and systematically lower than observed by Waclawska (1998). The differences in temperature could be related to the heating rates of the experiments because faster heating rates cause the reaction to appear at higher temperatures. Waclawska (1998) used a much slower heating rate at 2.5K/min compared to the 15K/min rate used in this study. Giese and Kerr (1959) did not report their heating rate.

Tincalconite's first reaction (endothermic) occurs at the same temperature as the third borax reaction (161 ºC), compared to Waclawska (1998) that observed this transition at 137ºC. The second peak (exothermic) occurs at 646ºC, suggesting the mineral becoming amorphous. Waclawska (1998) did not heat the experimental samples to that high of a temperature.

Kernite has two endothermic reactions; one at 165ºC and the other at 196ºC. Waclawska has the two endothermic reactions referenced previously at 155ºC and 159ºC, but has two earlier reactions at 84ºC and 100ºC in which the OH groups and water are split from the structure. The

first two reactions of kernite seen by Waclawska are not found in our TGA curves. This could be due to differences in the heating rate utilized by each scientist. There have been reports of another phase formed from the dehydration of kernite. Metakernite, Na2B4O6(OH)2•1.5H2O, has been formed from the heating of kernite by Muessig (1959) and Sennova, et al. (2005). Sennova et al.(2005) determined that this new phase consisted of the same chains (minus water molecules) that kernite did, which allow for a simple transition from kernite to meta-kernite. The two dehydration events, seen in the kernite TGA curve in the present study (Figure 3-1), result in the formation of meta-kernite (Sennova, 2005).

**Comparison with Previous Equilibrium Observations and Thermodynamic Results**

The results from experimental observations of this study for the dehydration of borax to tincalconite (Figure 3-4) are in good agreement with previous observations of this reaction. The curve in Figure 3-4 calculated from the thermodynamic properties derived in this study similarly agrees with previous observations. Our results confirm and extend the observations of Menzel(1935), Menzel and Schulz (1940), and Bowser (1965) on the T-RH conditions of reaction between borax and tincalconite (Figure 3-4). As temperature increases, tincalconite becomes increasingly stable with respect to borax at pure-$H_2O$-undersaturated conditions until it is the only phase stable in the presence of an aqueous solution.

The present study reports a series of new observations of the temperature dependence of $C_p$ for 1:2 sodium borates. The heat capacity of borax at 298.15K was determined to be ~586.5 J/molK; lower than evaluated by Wagman et al.(1982; 615 J/molK). The cause of this discrepancy is unclear. To my knowledge there are no previous determinations of $C_p$ for tincalconite or kernite. At 298.15K tincalconite's heat capacity is 367.45 J/molK and kernite is 337.32 J/molK (Table 1).

The results of the present study permit assessment of the properties of $C_p$ for the waters of hydration in borax that are lost during the conversion to tincalconite. Barrer (1978) reasoned that as water molecules adsorb into the structure of a mineral, such as a zeolite or other mineral hydrate, the loss of rotational and translational degrees of freedom in the crystal structure over those in an ideal gas should be manifest by an increase in Cp. His statistical mechanical model also predicts that for each of the six degrees of motional freedom (three translational and three rotational) lost to vibrational modes in the crystal during sorption, Cp should increase by 0.5 R (R is the gas constant; 8.314 J/molK) to a maximum of 3R. At 298.15K the average Cp of the water molecules in borax relative to tincalconite is 37.98J/molK per water molecule. This is an increase of ~0.5R over $C_p$ of $H_2O$ vapor, corresponding to a loss of one degree of motional freedom during incorporation of these water molecules into the borax structure.

The thermodynamic properties of borax, tincalconite, and kernite were calculated from the thermodynamic model and calorimetric experimental results. Previously, borax's properties had not been calculated from direct measurements, and very few thermodynamic properties for tincalconite and kernite had been published (Anovitz and Hemingway, 1996). Navrotsky et al. (unpublished; cited in by Anovitz and Hemingway, 1996) assessed $\Delta H_f^o$ of tincalconite calorimetrically through two different thermochemical cycles to be -4770.5kJ/mol (relative to boric acid) and -4785.1kJ/mol (relative to caliborite). Our value for $\Delta H_f^o$ was significantly lower at -4713.6kJ/mol. Their kernite $\Delta H_f^o$ is -4507.4 kJ/mol, while ours was -4580.19 kJ/mol. The discrepancies could be due to the difference in methods of measurement. Using the group contribution method (adding up thermodynamic properties of the individual ions in a mineral), Li et al. (2000) calculated the $\Delta H^0_f$ of borax, tincalconite, and kernite. The numbers they calculated were -6268.5 kJ/mol, -4816.4 kJ/mol, and -4506.21 kJ/mol respectively, compared to our values

of tincalconite and kernite at -4713.6 and -4580.19 kJ/mol, respectively. The $\Delta G^{o}_{f}$ of borax was reported by Bassett (1976) as -5516.60kJ/mol based on its solubility in water, compared to Wagman's value of -5516.02 kJ/mol. The group contribution method resulted in a borax $\Delta G^{0}_{f}$ of -5518.01 kJ/mol.

**Phase Relations between 1:2 Sodium Borates**

Figure 5-1 shows the calculated phase relations among 1:2 sodium borates calculated from the thermodynamic properties in Table 4-1. The solid line is representative of the transition between borax and kernite, where kernite is stable phase below the solid line while borax is stable above. The dotted line represents the transition between borax (stable above the line) and tincalconite (stable below the line). The three dots with the error bars are the equilibrium conditions of borax-tincalconite from the equilibrium observations. The error bar on the point at 298.15K intersects the borax-kernite curve representing the conditions where tincalconite could be a stable phase. The dashed line represents the RH of a saturated sodium borate solution (Blasdale and Slansky, 1939, and Menzel and Schulz, 1964), which is near the point of deliquesence. Blasdale and Slanksy (1939) and Menzel and Schulz (1940) report the borax-kernite transition occurs at 331.65K at 96.6% RH (star in Figure 5-1), while the transition of borax to tincalconite occurs at 333.95K (inverted triangle in Figure 5-1) (Christ and Garrels, 1959). In this purely $Na_2B_4O_7$-$H_2O$ system, borax and kernite are the stable phases at other temperatures and RH, therefore tincalconite is metastable (Christ and Garrels, 1959, and Bowser, 1965).

Figure 5-2 reveals the calculated phase relations seen in Figure 5-1, but now includes geologic observations from the Kramer Deposit in California of borax and tincalconite. Kernite is seen in the Kramer deposit at much greater depths (~ 1 km) (Christ and Garrels, 1959). When geothermal gradient is taken into account the temperature increases by ~ 33 km, therefore

pushing the tincalconite point seen in Figure 5-2 further into the kernite stability field. The NaCl saturated solution line is shown for reference because borate deposits often contain other salts such as NaCl. With the addition of NaCl, the relative humidity of the system would be decrease to the NaCl saturated solution line resulting in tincalconite or kernite becoming the stable phase.

With the addition of other ions in solution tincalconite's solubility is decreased due to the common ion effect, therefore allowing primary precipitation of tincalconite (Bowser, 1965). For instance, Pabst and Swayer (1948) report that if sulfate ions are introduced into solution, the tincalconite will form down to temperatures of 322.45K, but with the addition of sulfate and ammonium ions, the transition temperature lowers even further to 314.85K. They also predicted that in the presence of other additional ions tincalconite may precipitate at even lower temperatures. Bowser (1965) and Pabst and Sawyer (1948) have reported that other non-marine evaporite lakes, such as Searles Lake, have precipitated tincalconite out of solution (as a primary precipitate not a psuedomorph). This indicates that the tincalconite transition line is lowered and tincalconite becomes a stable phase at more than just 298.15K and 65% RH. The Kramer deposit, the world's largest and most important source of Na-borates in the world is free of the other salty sediments found elsewhere (Bowser, 1965; Muessig and Allen, 1957). Without significant amounts of other ions, the Kramer borates are chemically similar to the phase diagram (Figure 5-1).

As was stated by Christ and Garrels (1959), the reaction between the minerals is a function of temperature, pressure, and vapor pressure of water (relative humidity). The reaction between borax and kernite can be dependent on the energy associated with the reaction and chemical arrangement. The reversible reaction from borax to tincalconite (and vice versa) occurs rapidly at surface conditions, while the borax to kernite reaction takes much more time with

increased temperature and pressure (Christ and Garrels, 1959; Bowser, 1965). Borax and tincalconite both contain the polyanion $[B_4O_5(OH)_4]^{-2}$ and therefore can convert rapidly to each other with little energy associated with the reaction (loss/gain of water)(Christ and Garrels, 1959;Morimoto, 1956). Christ and Garrels (1959) calculated the pressure (depth) based on geothermal gradient and temperature associated with the borax to kernite reaction to be 2500±500 feet. Kernite differs in that it contains chains of $[B_4O_6(OH)_2]_n^{-2n}$ polyanions, resulting in the polymerization reaction of $n[B_4O_5(OH)_4]^{-2} = [B_4O_6(OH)_2]_n^{-2n} + nH_2O$ requiring appreciable activation energy (Christ and Garrels, 1959). Blasdale and Slansky (1939), as well as Menzel and Schulz (1940), produced a solubility- temperature curve for the system $Na_2B_4O_7$-$H_2O$ in which the transition point for borax to kernite occurs at 58.5 ºC, while the borax to tincalconite occurs at 60.8 ºC. From the experimental observations we observe tincalconite as the secondary mineral that forms at both of these temperatures. Because of the structure and activation energy needed in the transformation from borax to kernite, tincalconite forms instead (meatastably).

Borax is described as a primary evaporite because it is most often the first of the Na-suite to form at surface conditions (Muessig, 1959). Muessig (1959) describes primary borate evaporites as minerals that form at the lowest temperatures under surface conditions of playas, also having the lowest specific gravity and hence the highest water content. Because tincalconite psuedomorphs borax where it has been exposed to dry desert air and then transforms back to borax when re-exposed to moisture (Christ and Garrels, 1959), tincalconite was formally described as secondary and metastable, but now can be described as primary and stable (Figure 5-1). Kernite is regarded as a secondary mineral in the $Na_2B_4O_7$-$H_2O$ system; a product of thermal diagenesis of borax. Kernite is seen deep in the Kramer deposit in irregularly shaped masses, indicative of secondary mineralization (Christ and Garrels, 1959). The transformation

from kernite back to borax occurs when kernite is exposed to weathering (Warren, 1999), confirming that borax is a stable phase at surface conditions. This was also seen in our laboratory experiments where kernite was left in a 97% RH environment at 25ºC for 3 months resulting in borax.

## Other Borate Systems

The findings from this investigation of Na-borates can be applied to other borate systems (Ca, Mg, NaCa). The calcium borate suite mirrors the sodium suite with a high, mid, and low hydrate. Inyoite [$Ca_2B_6O_{11}$•$13H_2O$] and myerhoffite [$Ca_2B_5O_{10}$•$7H_2O$] contain the polyanion $[B_3O_3(OH)_5]^{-2}$. Colemanite [$Ca_2B_5O_{11}$•$5H_2O$], like kernite, contains chains of polyanions, but of the composition $[B_3O_4(OH)_3]_n^{-2n}$. The polymerization reaction is $n[B_3O_3(OH)_5]^{-2} = [B_3O_4(OH)_3]_n^{-2n} + n\ H_2O$ (Christ and Garrels, 1959). The similarities in the two reactions of borax to kernite and inyoite to colemanite make the study of the Na-system important to the Ca-system.

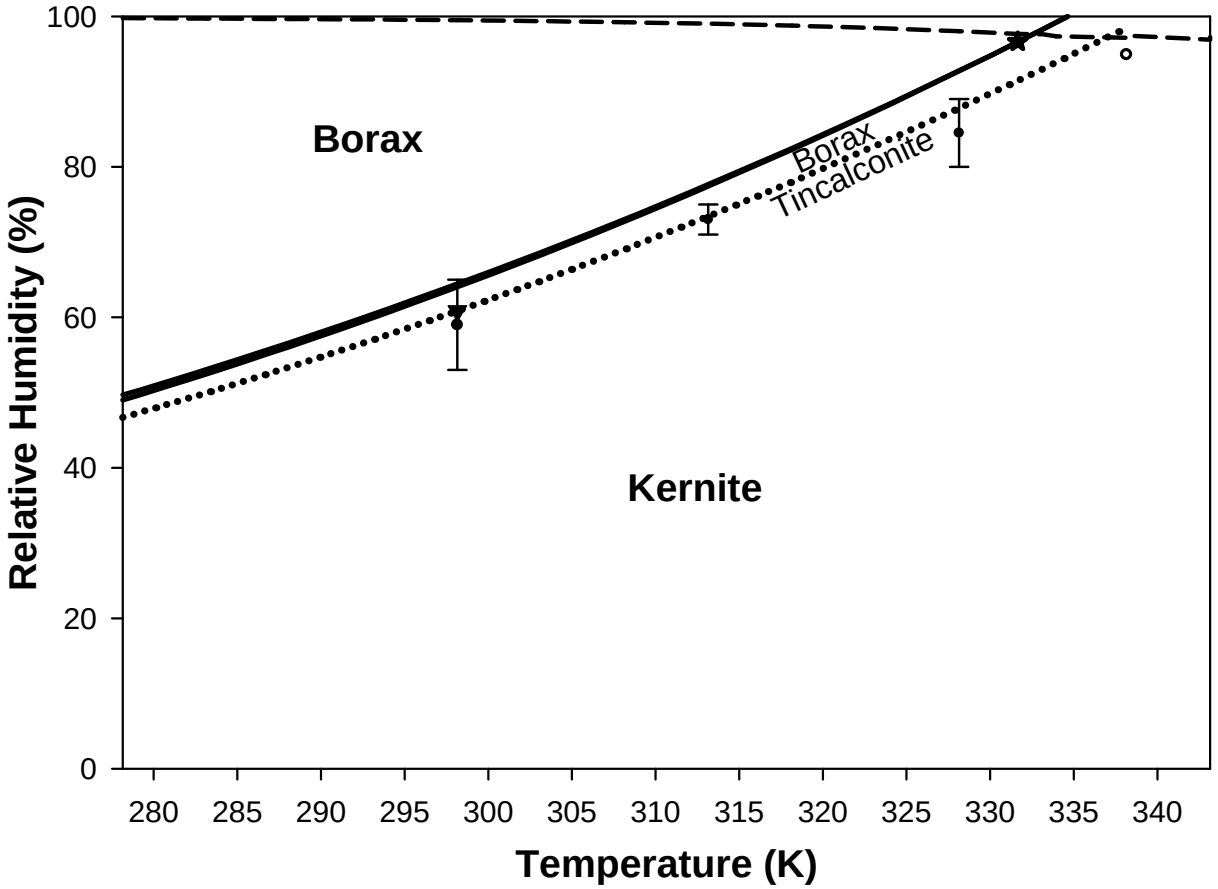


Figure 5-1. Phase diagram of borax, tincalconite, and kernite. The solid line represents equilibrium between borax and kernite, while the dashed line represents equilibrium between borax and tincalconite. The star represents the borax-kernite transition recognized by Menzel and Schulz (1940) and Blasdale and Slansky (1939). The inverted triangle is the transition of borax to tincalconite recognized by Christ and Garrels (1959). The open circle is the point of deliquescence and the dashed line is the RH of a saturated sodium borate solution. The dots with error bars are the equilibrium between borax and tincalconite realized in the equilibrium observations.

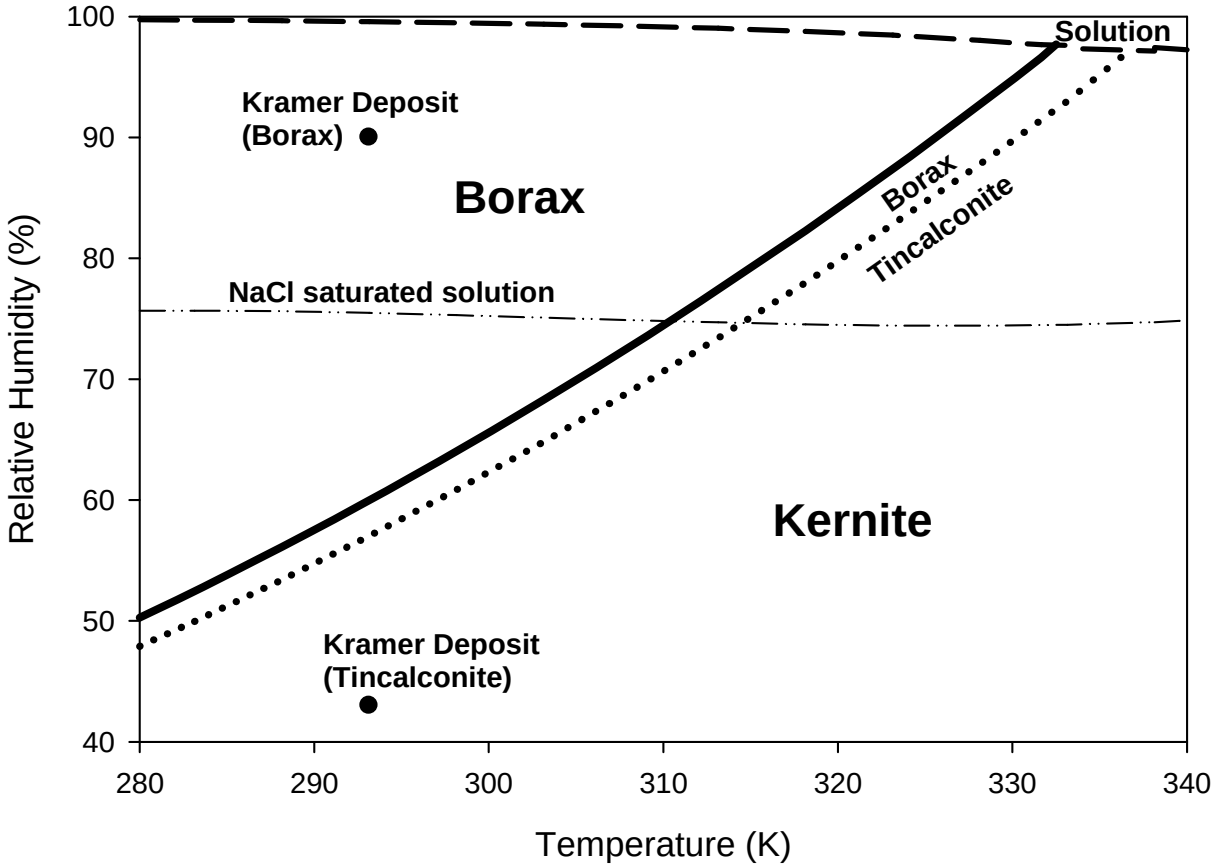


Figure 5-2. Phase diagram with geologic observations of borax, tincalconite, and kernite. The solid line represents equilibrium between borax and kernite, while the dashed line represents equilibrium between borax and tincalconite. The thick dashed line is the RH of a saturated sodium borate solution. Geologic observations from the Kramer Deposit, California match the stability fields of borax and tincalconite shown in the phase diagram. The NaCl saturated solution line is shown for reference, revealing the RH of a system saturated with NaCl as seen in some borate deposits.

# CHAPTER 6
# CONCLUSIONS

This suite of sodium borate minerals is very important economically, therefore understanding their stability and formation is of the utmost importance. Through experimental observations, the stability of borax and tincalconite were established in the $Na_2B_4O_7$-$H_2O$ system. Borax seems to be the primary precipitate in the $Na_2B_4O_7$-$H_2O$ system, but tincalconite does have a small stability field at 298.15K and 65%. Kernite is a thermal diagenesis product of borax. With the addition of other ions, the solubility of tincalconite and kernite are lowered allowing them to become a stable phase and precipitate directly from solution as seen at Searles Lake. The differences in structure between borax, tincalconite, and kernite were discussed to help explain the difficulty in transformation to kernite. Due to the similarities in the structure and behavior, these findings can be applied to other borate systems, like the Ca, Na-Ca, and Mg-borates.

The TGA curves from each mineral confirm the structure and water content of the minerals. TGA measurements and equilibrium observations confirm the best stoichiometry of tincalconite as $Na_2B_4O_5(OH)_4 \bullet 2.667H_2O$. Through HF calorimetry, DSC-TGA analysis, X-ray diffraction, and equilibrium experiments the thermodynamic properties of these borax, tincalconite, and kernite ($Cp^o$, $\Delta H_f^o$, $S^o$, $\Delta G_f^o$ at 298.15 K) were measured and calculated using the thermodynamic model. The heat capacity of the hydration reaction is equal to 0.5R which reveals that one degree of motional freedom among the water molecules was lost.

LIST OF REFERENCES

Anovitz, L. and Grew, E. (1996) Introduction. Reviews in Mineralogy, 33, 263-298.

Anovitz, L. and Hemingway, B. (1996) Thermodynamics of boron minerals: summary of structural, volumetric, and thermochemical data. Reviews in Mineralogy, 33, 181-262.

Barrer, R.M. (1978) Zeolites and clay minerals as sorbents and molecular sieves, 497p. Academic Press, London.

Bassett, R. L. (1976) The geochemistry of boron in thermal waters: Ph.D. dissertation, Stanford University, Stanford, California, 290.

Benson, S.W. (1968) Thermochemical kinetics. New York, Jon Wiley and Sons, 233.

Bixler, G.H. and Sawyer, D.L. (1957) Boron chemicals from Searles Lake brines. Industrial and Engineering Chemistry, 49, 322-333.

Blasdale W.C. and Slansky, C.M. (1939) The solubility curves of boric acid and the borates of sodium. Journal of the American Chemical Society, 61, 917-920.

Bowser, C. J. (1965) Geochemistry and petrology of the sodium borates in the non-marine evaporite environment; dissertation UCLA; 1964-65

Bowser, C.J. (1965) Origin of tincalconite at Searles Lake, CA. American Mineralogist, 50, 281.

Burns, P.C., Grice, J.D., and Hawthorne, F.C. (1995) Borate Minerals. I. Polyhedral clusters and fundamental building blocks. The Canadian Mineralogist, 33, 1131-1151.

Cammenga, H.K., Eysel, W., Gmelin, E., Hemminger, W., Höhne, G.W.H., and Sarge, S.M. (1993) The Temperature Calibration of Scanning Calorimeters. 2. Calibration Substances. Thermochimica Acta, 219, 333-342.

Chirife, J. and Resnik, S. (1984) Unsaturated solutions of sodium chloride as reference sources of water activity at various temperatures. Journal of Food Science, 49, 1486-1488.

Christ, C. and Garrels, R. (1959) Relations among sodium borate hydrates at the Kramer Deposit, Boron, CA. American Journal of Science, 257, 516-528.

Chou, M., Seal II, R., and Hemingway, B. (2002) Determination of melanterite-rozenite and chalcanthite-bonattite equilibria by humidity measurements at 0.1 MPa. American Mineralogist, 87, 108-114.

Cooper, W.F., Larsen, F.K., Coppens, P., and Giese, R.F. (1973) Electron population analysisof accurate diffraction data; V structure and once center charge refinement of the light-atom mineral kernite $Na_2B_4O_6(OH)_2 \bullet 3H_2O$. American Mineralogist, 58, 21-31.

Dickson, A.G. (1990) Thermodynamics of the dissociation of boric acid in synthetic seawater from 273.15 to 318.15 K. Deep-Sea Res., 37, 755–766.

Distanov, E.G. and Kopeikin, V.A. (1990) Analysis of calculation of thermodynamic characteristics of borates based on solubility data. Dokl Akad Nauk SSSR, 312, 958-962.

Downs, R.T. (2005) XtalDraw for Windows. Commission on Powder Diffraction, International Union of Crystallography Newsletter 30, 32-33.

Eugster, H.P. and Smith, G. I. (1965) Mineral equilibria in the Searles Lake evaporites, California. Journal of Petrology, 6, 473-522.

Giacovazzo, C., Menchetti, S., and Scordari, F. (1973) Crystal structure of tincalconite. American Mineralologist, 58, 523-530.

Giese,R.F. Jr. (1966) Crystal Structure of Kernite, $Na_2B_4O_6(OH)_2 \bullet 3H_2O$. Science, 154, 1453-1454.

Giese, R.F. Jr., and Kerr, P.F. (1959) Thermal reactions of hydrated sodium tetraborates, Geological Society of America Bulletin, 70, 1608-1609.

Gmelin, E. and Sarge, S.M. (2000) Temperature, heat and heat flow rate calibration of differential scanning calorimeters. Thermochimica Acta.347, 9-13.

Greenspan, L. (1977) Humidity fixed points of binary saturated aqueous solutions, Journal of research of the national Bureau of Standards-A. Physics and Chemistry, 81A, 1.

Grice, J.D., Burns, P.C., and Hawthorne, F.C. (1999) Borate Minerals. II. A hierarchy of structures based upon the borate fundamental building block. The Canadian Mineralogist, 37, 731-762.

Helgeson, H.C., Delany, J.M., Nesbitt, H.W., and Bird, D.K. (1978) Summary and critique of the thermodynamic properties of rock-forming minerals. American Journal of Science, 278, 1-229.

Helvaci, C. and Orti, F. (2004) Zoning in the Kirka borate deposit, western Turkey; primary evaporitic fractionation or diagenetic modifications?, The Canadian Mineralogist, 42, 1179-1204.

Höhne, G.W.H., Cammenga, H.K., Eysel, W., Gmelin, E., and Hemminger, W. (1990) The Temperature Calibration of Scanning Calorimeters. Thermochimica Acta, 160, 1-12.

Hovis, G.L., Roux, J., and Richet, P. (1998) A new era in hydrofluoric acid solution calorimetry; reduction of required sample size below ten milligrams, American Mineralogist, 83, 931-934.

Hovis, G.L. and Roux, J. (1993) Thermodynamic mixing properties of nepheline-kalsilite crystalline solutions, American Journal of Science, 293, 1108-1127

Hurlbut, C.S. Jr., Aristarain, L.F., and Erd, R.C. (1973) Kernite from Tincalayu, Salta, Argentina. American Mineralogist, 58, 308-313.

Inan, K., Dunham, A.C., and Esson,J. (1973) Mineralogy, chemistry and origin of Kirka borate deposit, Eskisehir Province, Turkey, Trans. Inst. Mining Metall., 82B, 114–123.

Kemp, P.H. (1956) The Chemistry of Borates; Part 1. Borax Consolidated Limited, London.

Krauskopf, K. and Bird, D. (1995) Introduction to Geochemistry, 3rd ed., McGraw-Hill, New York.

Leeman, W.P. and Sission, V.B. (1996) Geochemistry of boron and its implications for crustal and mantle processes, Reviews in Mineralogy, 33, 645-707

Levy, H. A. and Lisensky, G. C. (1978) Crystal structures of sodium sulfate decahydrate (Glauber's salt) and sodium tetraborate decahydrate (borax): Redetermination by neutron diffraction. Acta Crystallographica B34, 3502-3510.

Li, J., Li, B., and Gao, S. (2000) Calculation of thermodynamic properties of hydrated borates by group contribution method. Physical Chemical Minerals, 27, 342-346.

Luck, R. and Wang, G. (2002) On the nature of tincalconite. American Mineralogist, 87, 350-354.

Maier, C.G. and Kelley, K.K. (1932) An equation for the representation of high-temperature heat content data. Journal of the American Chemical Society, 54, 3243-3246.

Menzel, H.(1935) Information on boric acids and boric acid alkali salts IX The system Na2B4O7-H2O. Zeitschrift Fur Anorganische und Allgemeine Chemie, 224, 1-22.

Menzel, V. and Schulz, H. (1940) Der Kernit (Rasorit)Na2B4O7•4H2O. Zeitschrift fur anorganische und allgemeine Chemie, 245, 157-220.

Morimoto, N. (1956) The crystal structure of borax. Mineral Journal of Japan, 2, 1.

Muessig, S.J. and Allen, R.D. (1957) The hydration of kernite ($Na_2B_4O_7$•$4H_2O$). American mineralogist, 42, 699-701.

Muessig, S.J. (1959) Primary borates in playa deposits; minerals of high hydration. Economic Geology and the Bulletin of the Society of Economic Geologists, 54, 3, 495-501.

Neuhoff, P.S, Wang, J. (2007) Heat capacity of hydration in zeolites. American Mineralogist, 92, 1358-1367

Neuhoff, P.S. and Wang, J. (2007) Isothermal measurement of heats of hydration in zeolites by simultaneous thermogravimetry and differential scanning calorimetry. Clays and Clay Minerals, 55, 239-252.

Pabst, A. and Sawyer, D.L. (1948) Tincalconite crystals from Searles Lake, San-Bernardino County, CA. American Mineralogist, 33, 472-481.

Palache, C., Berman, H., and Frondel, C. (1951) Dana's System of Mineralogy, 7th ed., Wiley, New York.

Powell, D.R., Gaines, D.F., Zerella, P.J., and Smith, R.A. (1991) Refinement of the structure of tincalconite. Acta Crystallographica, C47, 2279-2282.

Price, D.M. (1995) Temperature calibration of differential scanning calorimeters. Journal of Thermal Analysis, 45, 1285-1296.

Ricardo, A. Carrigan, M., Olcott, A, and Benner, S. (2004) Borate minerals stabilize ribose. Science, 303, 196.

Robie, R.A. and Hemingway, B.S. (1995) Thermodynamic properties of minerals and related substances at 298.15K and 1bar ($10^5$ pascals) pressure and at higher temperatures. US Geological Survey Bulletin, 2131, 416.

Sabbah, R., An, X.W., Chickos, J.S., Leitao, M.L.P., Roux, M.V., and Torres, L.A. (1999) Reference materials for calorimetry and differential thermal analysis. Thermochimica Acta, 331, 93-204.

Sarge, S.M., Gmelin, E., Höhne, G.W.H., Cammenga, H.K., Hemminger, W., and Eysel, W. (1994) The Caloric Calibration of Scanning Calorimeters. Thermochimica Acta, 247, 129-168.

Schaller, W.T. (1936) The origin of kernite and borax in the Kramer borate field, California, American Mineralogist, 21, 192.

Sennova, N.A., Bubnova, R.S., Filatov, S.K., Paufler, P., Meyer, D.C., Levin, A.A., and Polyakova, I.G. (2005) Room, low, and high temperature dehydration and phase transitions of kernite in vacuum and air. Crystal Research and Technology, 40, 563-572.

Smith G. and Medrano M. (1996) Continental borate deposits of Cenozoic age. Reviews in Mineralogy, 33, 263-298.

Stølen, S., Glockner, R., and Grønvold, F. (1996) Heat capacity or the reference material synthetic sapphire (alpha-Al2O3) at temperatures from 298.15 K to 1000 K by adiabatic calorimetry. Increased accuracy and precision through improved instrumentation and computer control. Journal of Chemical Thermodynamics, 28, 1263-1281.

Waclawska, I. (1998) Controlled rate thermal analysis of hydrated borates. Journal of Thermal Analysis, 53, 519-532.

Waldbaum, D.R. and Robie, R.A. (1970) An internal sample container for hydrofluoric acid solution calorimetry, Journal of Geology, 78, 736-741.

Wagman D.D., Evans, W.H., Parker, V.B., Schumm, R.H., Halow, I, Bailey, S.M., Churney, K.L., and Nuttall, R.L. (1982) The NBS tables of chemical thermodynamic properties: Selected values for inorganic and $C_1$ and $C_2$ organic substances in SI units. Journal of Physical Chemistry Reference, 11, 2.

Wagner, W. and Pruß, A. (2002) The IAPWS formulation 1995 for the thermodynamic properties of ordinary water substance for general and scientific use. Journal of Physical and Chemical Reference Data, 31, 387-535.

Warren, J.K. (1999) Evaporites: Their Evolution and Economics. Blackwell Science, Malden, MA.

Warren, J.K. (2006) Evaporites: Sediments, Resources, and Hydrocarbons. Springer, Berlin, NewYork.

Woods, W. (1994) An introduction to boron: history, sources, uses, and chemistry. Environmental Health Perspectives, 102, 7.

# BIOGRAPHICAL SKETCH

Laura was born in Monroe, Louisiana, and grew up there and in Ft. Myers, FL. She attended Ft. Myers High School and completed the International Baccalaureate program. Afterward, she attended the University of Florida, just as her grandfather, father, aunt, and uncle did. She earned a Bachelor of Science degree in geological sciences in 2006. Laura decided to continue her education at the University of Florida and worked on her Master of Science in geology under the direction of Philip Neuhoff. While at the University of Florida Laura has maintained many great friendships and taken part in many extracurricular activities, thoroughly enjoying her time as a gator.